



## Extended late Holocene relative sea-level histories for North Carolina, USA



Andrew C. Kemp<sup>a,\*</sup>, Jessica J. Kegel<sup>b</sup>, Stephen J. Culver<sup>b</sup>, Donald C. Barber<sup>c</sup>, David J. Mallinson<sup>b</sup>, Eduardo Leorri<sup>b</sup>, Christopher E. Bernhardt<sup>d</sup>, Niamh Cahill<sup>e</sup>, Stanley R. Riggs<sup>b</sup>, Anna L. Woodson<sup>b,c</sup>, Ryan P. Mulligan<sup>f</sup>, Benjamin P. Horton<sup>g,h</sup>

<sup>a</sup> Department of Earth and Ocean Sciences, Tufts University, Medford, MA 02155, USA

<sup>b</sup> Department of Geological Sciences, East Carolina University, Greenville, NC 27858, USA

<sup>c</sup> Department of Geology, Bryn Mawr College, Bryn Mawr, PA 19010, USA

<sup>d</sup> United States Geological Survey, National Center 926A, Reston, VA 20192, USA

<sup>e</sup> Department of Biostatistics and Epidemiology, University of Massachusetts Amherst, Amherst, MA 01003, USA

<sup>f</sup> Department of Civil Engineering, Queen's University, Kingston, Ontario, Canada

<sup>g</sup> Institute of Coastal and Marine Sciences, Rutgers University, New Brunswick, NJ 08901, USA

<sup>h</sup> Earth Observatory of Singapore and Asian School of the Environment, Nanyang Technological University, 639798, Singapore

### ARTICLE INFO

#### Article history:

Received 25 October 2016

Received in revised form

15 January 2017

Accepted 19 January 2017

Available online 7 February 2017

#### Keywords:

Foraminifera

Gulf Stream

Tidal-range change

Salt marsh

### ABSTRACT

We produced ~3000-year long relative sea-level (RSL) histories for two sites in North Carolina (USA) using foraminifera preserved in new and existing cores of dated salt-marsh sediment. At Cedar Island, RSL rose by ~2.4 m during the past ~3000 years compared to ~3.3 m at Roanoke Island. This spatial difference arises primarily from differential GIA that caused late Holocene RSL rise to be 0.1–0.2 mm/yr faster at Roanoke Island than at Cedar Island. However, a non-linear difference in RSL between the two study regions (particularly from ~0 CE to ~1250 CE) indicates that additional local- to regional-scale processes drove centennial-scale RSL change in North Carolina. Therefore, the Cedar Island and Roanoke Island records should be considered as independent of one another. Between-site differences on sub-millennial timescales cannot be adequately explained by non-stationary tides, sediment compaction, or local sediment dynamics. We propose that a period of accelerating RSL rise from ~600 CE to 1100 CE that is present at Roanoke Island (and other sites north of Cape Hatteras at least as far as Connecticut), but absent at Cedar Island (and other sites south of Cape Hatteras at least as far as northeastern Florida) is a local-to regional-scale effect of dynamic ocean and/or atmospheric circulation.

© 2017 Elsevier Ltd. All rights reserved.

### 1. Introduction

During the late Holocene (here defined as the past ~3000 years) relative sea-level (RSL) change on the Atlantic coast of North America was driven by processes such as glacio-isostatic adjustment (GIA; e.g., Peltier, 1996), changes in ocean mass and volume (adjusted where necessary for its source-dependent fingerprint; e.g., Mitrovica et al., 2001, 2011), redistribution of existing ocean mass by ocean and atmospheric circulation (termed “ocean dynamics”; e.g., Ezer et al., 2013; Levermann et al., 2005; Piecuch et al., 2016) and tidal-range change (e.g., Hill et al., 2011) that varied spatially and on timescales from decades to millennia. These

processes produced a complex, spatio-temporal pattern of local RSL histories that can be reconstructed using proxies preserved in salt-marsh sediment (e.g., foraminifera; Edwards and Wright, 2015; Scott and Mediolli, 1978). Such RSL reconstructions provide a near-continuous time series with relatively small vertical and temporal uncertainties. This resolution enables contributions to RSL trends from specific processes to be estimated (or indeed discounted) by comparing and contrasting RSL histories across a suite of sites (e.g., Kemp et al., 2014; Long et al., 2014). The most precise RSL reconstructions are generated in depositional environments with small tidal ranges (Barlow et al., 2013).

Estuaries enclosed by the Outer Banks of North Carolina (USA; Fig. 1) are ideal places to produce late Holocene RSL reconstructions because the region is characterized by great diurnal tidal ranges (mean lower low water, MLLW, to mean higher high water, MHHW) that are often less than 0.2 m and their expansive salt marshes are

\* Corresponding author.

E-mail address: [andrew.kemp@tufts.edu](mailto:andrew.kemp@tufts.edu) (A.C. Kemp).

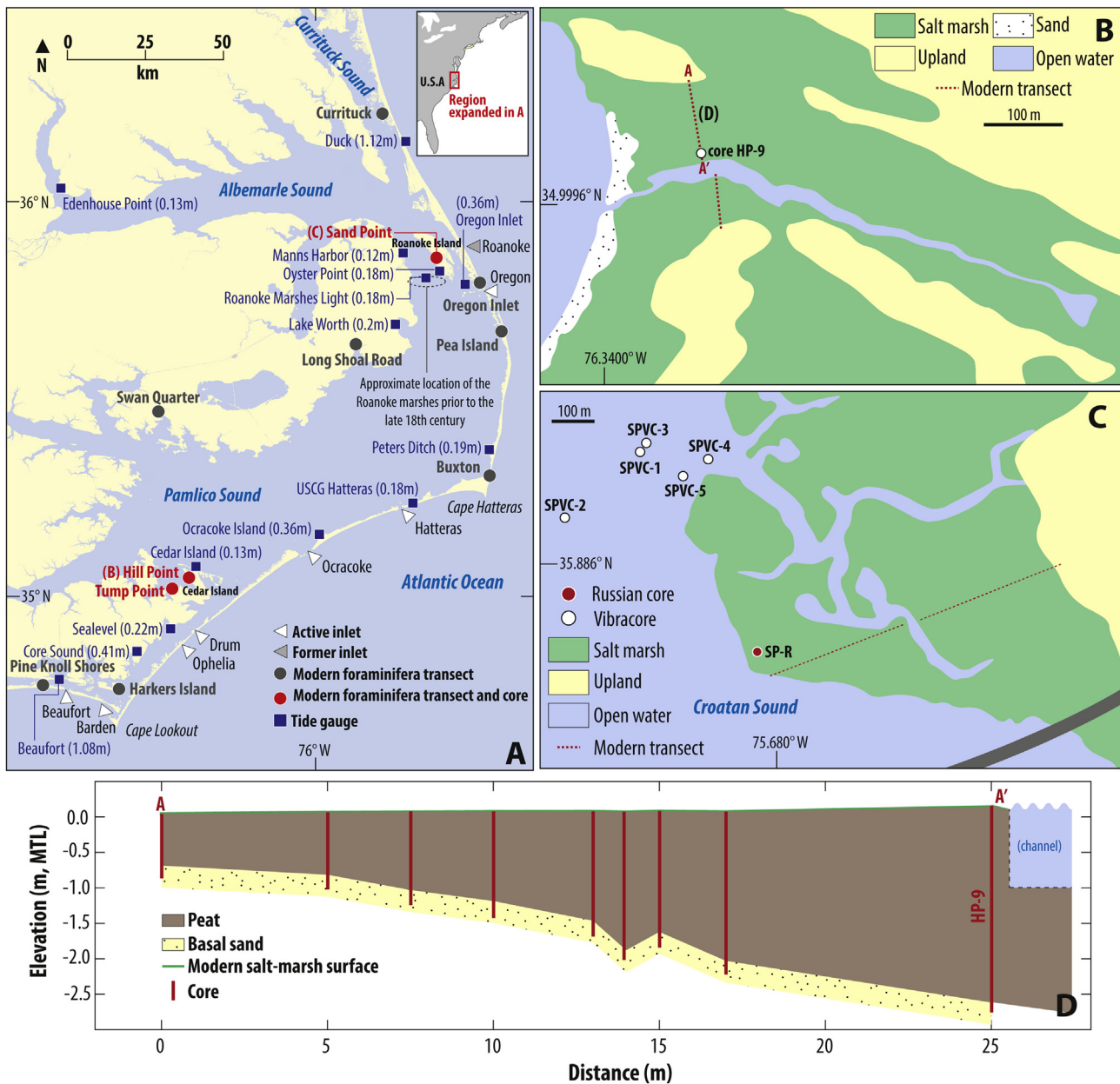


**Fig. 1.** Study region in North Carolina, U.S.A. (A) Cores of salt-marsh sediment used to reconstruct relative sea level (RSL) are from the Sand Point, Hill Point and Tump Point sites. The distribution of modern foraminifera was documented at eleven sites. The location of select tide gauges (including those referred to in the main text) are shown with their reported great diurnal tidal range in parentheses. Roanoke Inlet is just one of many previous inlets, but is shown because of its importance for evaluation of Croatan Sound and the Roanoke Marshes. (B) Core HP-9 was recovered from Hill Point and extends the Tump Point RSL record of Kemp et al. (2011). (C) Core SPVC-2 in Croatan Sound extends the Sand Point RSL reconstruction of Kemp et al. (2011) that was developed from a Russian core (SP-R). (D) Stratigraphy underlying the salt marsh at Hill Point described from a series of cores (including HP-9) positioned along transect A-A'. The transect was ended (A') at the edge of an active tidal channel that was likely cut into the sedimentary record (dashed lines represent uncertain and possibly erosive channel margins).

underlain by thick and continuous late Holocene sequences of salt-marsh peat. These factors motivated Kemp et al. (2011, 2009c) to reconstruct RSL at Tump Point since ~1100 CE and at Sand Point since ~100 BCE (Fig. 1). Agreement between these records, following correction for the estimated contribution from GIA, indicated that they represented regional-scale sea-level trends in a key location for understanding physical processes that vary along latitudinal gradients in the Atlantic Ocean, such as GIA (e.g., Peltier, 1996), the fingerprint of Greenland Ice Sheet melt (e.g., Mitrovica et al., 2001), and ocean dynamics (e.g., Yin and Goddard, 2013). However, the period prior to ~1100 CE is represented solely by the Sand Point reconstruction and geological evidence for opening/closing

of the Outer Banks barrier (e.g., Grand Pre et al., 2011; Mallinson et al., 2010, 2011; Moran et al., 2015; Zaremba et al., 2016) suggests that tidal-range change could have influenced spatial patterns of RSL change within North Carolina during this time period. It is unclear, therefore, how well regional RSL trends (and their causes) before ~1100 CE are represented by the existing reconstruction from Sand Point.

Our goal is to extend the existing late Holocene RSL reconstructions to better understand the spatial pattern and causes of sea-level variability within North Carolina and along the Atlantic coast of North America with particular emphasis on the period prior to ~1100 CE. We extended the existing Tump Point record by

reconstructing RSL from ~1000 BCE to ~1500 CE using a core of salt-marsh peat from a new site at Hill Point (Fig. 1). A new sediment core collected in Croatan Sound spans the period from ~1000 BCE to ~500 CE and is an extension of the Sand Point record. This analysis provides a near-continuous, ~3000 year-long sea-level history for two study areas (Cedar Island and Roanoke Island) in North Carolina that are located more than 100 km apart. We find that centennial-scale differences in RSL between these sites cannot be adequately resolved by tidal-range change and we treat the two records as independent of one another. We interpret the spatial pattern of RSL change within North Carolina and along the U.S. Atlantic coast as evidence for changes in ocean circulation and/or persistent trends in atmospheric pressure and circulation.

## 2. Study area and existing relative sea-level reconstructions

Our study area encompasses the coast of North Carolina from Currituck Sound to Cape Lookout, which is characterized by a chain of barrier islands (the Outer Banks) that separate the open Atlantic Ocean from back-barrier estuaries such as Pamlico Sound and Albemarle Sound (Fig. 1). Exchange of water between the estuaries and the Atlantic Ocean occurs through dynamic inlets which open, close and migrate through time (e.g., Culver et al., 2007; Mallinson et al., 2010, 2011). Great diurnal tidal range on the ocean side of the barrier islands is considerably larger (e.g., 1.12 m at Duck) than on the estuary sides (e.g., 0.36 m at Oregon Inlet and Ocracoke Island; Fig. 1). Within the estuaries, tidal ranges are even smaller at locations further away from open inlets (e.g., 0.12 m at Mann's Harbor, 0.13 m at Cedar Island and 0.18 m at Roanoke Marshes Light, Oyster Point and USCG Hatteras; Fig. 1), although prevailing winds cause elevations above highest astronomical tide (HAT) to be regularly inundated by salt water (e.g., Reed et al., 2008).

Salt marshes are found in protected back-barrier settings along the Outer Banks and on extensive platforms in the estuaries. Tidal flats are rare and low salt-marsh vegetation zones defined by *Spartina alterniflora* (tall form) are usually narrow (less than 10 m) in extent and are absent altogether at many sites where the erosive platform edge is demarcated by a step-change in elevation. Sediment in this low salt-marsh zone is composed of organic silt and clay. High salt-marsh vegetation communities are dominated by *Juncus roemerianus*, although patches of *Distichlis spicata* and *Spartina patens* are found at some sites. This zone can extend for several kilometers across low-relief platforms and is characterized by salt-marsh peat formation (typically 30–60% organic content as measured by loss on ignition; e.g., Brain et al., 2015; Brinson, 1991) in which macrofossils are abundant. The transitional zone from salt marsh to freshwater upland is commonly occupied by *Juncus roemerianus*, *Iva frutescens*, *Spartina cynosuroides*, *Cladium jamaicense*, *Schoenoplectus* spp. and/or *Phragmites australis* (e.g., Adams, 1963; Brinson, 1991; Eleuterius, 1976a; Kemp et al., 2010; Woerner and Hackney, 1997). The distribution of modern (surface) foraminifera on eleven salt marshes in the study region (Fig. 1) was described by Culver and Horton (2005), Horton and Culver (2008), Kegel (2015) and Kemp et al. (2009b) who demonstrated that foraminifera could be used as sea-level indicators, but that the composition of high salt-marsh assemblages varied among sites in response to salinity. The modern training set generated from these studies includes 205 samples and shows that high salt-marsh zones are populated by high, but variable, abundances of *Haplophragmoides wilberti*, *Trochammina inflata*, *Arenoparrella mexicana*, *Jadammina macrescens* and *Tiphrotrocha comprimata*. Therefore, down core switches among high salt-marsh assemblages likely reflect local paleoenvironmental changes in factors such as salinity, but not significant changes in tidal elevation. Low salt-marsh zones are dominated by *Miliammina fusca* and *Ammobaculites* spp.

Existing and near-continuous RSL reconstructions produced from salt-marsh sediment at Tump Point in Pamlico Sound and Sand Point in Croatan Sound (core SP-R; Fig. 1) show a continuous RSL rise during the past ~2000 years (Kemp et al., 2011). The Tump Point record had an average chronological uncertainty of  $\pm 39$  years ( $\sim 2\sigma$ ) and an average vertical uncertainty of  $\pm 0.03$  m ( $\sim 1\sigma$ ), but was hindered by systematically large chronological uncertainties prior to ~1100 CE ( $\sim 1.10$  m depth). The Sand Point reconstruction spanned the period from ~100 BCE to 1975 CE with an average chronological uncertainty of  $\pm 36$  years ( $\sim 2\sigma$ ) and an average vertical uncertainty of  $\pm 0.06$  m ( $\sim 1\sigma$ ). The interval since ~1975 CE is represented by a surface sand layer (Fig. 2) that was not used in the RSL reconstruction.

The new study site at Hill Point is located on Cedar Island ~4.5 km northeast of Tump Point (Fig. 1). It was selected after exploratory coring revealed it to have one of the thickest accumulations of salt-marsh peat (~2.2 m) in the region that was likely to overlap with and extend the existing RSL reconstruction from Tump Point. The sampled salt marsh lies on the edge of a tidal creek and behind a small beach and dune system. *Juncus roemerianus* is the dominant plant species and covers the entire site except for a narrow band of *Spartina alterniflora* along the creek banks. Results from two modern transects show that *Tiphrotrocha comprimata* is the dominant species of foraminifera (average 28%, up to 83%) at the site (Kegel, 2015).

The Sand Point site on Roanoke Island is a wide (up to 1.1 km) salt marsh almost exclusively vegetated by *Juncus roemerianus* with a narrow band of *Spartina alterniflora* on the edge of Croatan Sound. In the past, this marsh and interspersed tidal channels extended across present-day Croatan Sound to connect Roanoke Island to the mainland (e.g., O'Connor et al., 1972; Riggs and Ames, 2003; Riggs et al., 2000). Closure of Roanoke Inlet beginning in the late 18th century (and complete by 1817 CE; e.g., Mallinson et al., 2008) rerouted discharge from Albemarle Sound through Croatan Creek (situated to the east of Roanoke Island) and into the Pamlico basin. This reorganization overtopped the interstream divide at Roanoke Marshes, resulting in flooding and erosion (vertical and lateral) of the salt marsh that continues today. Remnants of the salt-marsh peat that accumulated in the Roanoke Marshes are preserved in the sedimentary record beneath Croatan Sound. This sediment represents an opportunity to extend the Sand Point RSL reconstruction beyond the record that lies beneath the modern salt marsh.

## 3. Methods

### 3.1. New cores

At Hill Point (Fig. 1B, D) we documented the stratigraphy underlying the modern salt marsh using a series of hand-driven cores (Eijkelpamp peat sampler; commonly called a "Russian" corer) positioned along a transect extending from the lower edge of the salt marsh adjacent to a tidal channel to the transition into an upland environment. Previous investigations by Barber and Woodson examined sedimentary successions at other locations beneath the Hill Point site and concluded that the transect location that we examined was representative of the site. In the field, sedimentary units were described and classified using the Troels-Smith (1955) system. Core HP-9 was selected for detailed analysis because it provided the deepest (and likely oldest) sequence of high salt-marsh peat and was representative of the site. The core was collected in overlapping 0.5-m intervals using an Eijkelpamp peat sampler to prevent compaction or contamination during collection. Each interval was transferred to a rigid plastic sleeve, wrapped in plastic and stored in refrigerated conditions until the time of

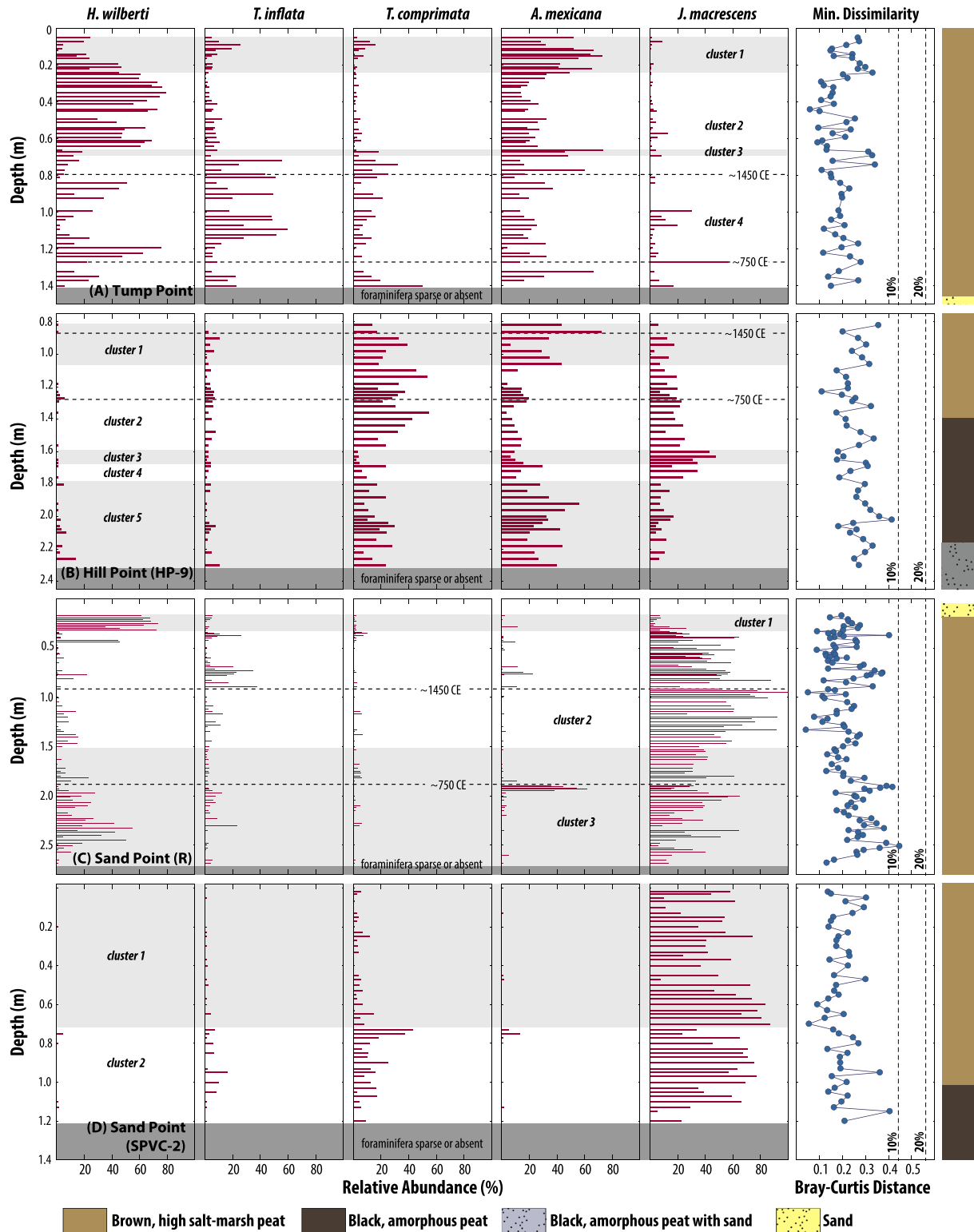


**Fig. 2.** Foraminifera preserved in cores of salt-marsh sediment from (A) Tump Point (Kemp et al., 2011), (B) Hill Point (HP-9; this study), (C) Sand Point Russian core (Kemp et al., 2011), and (D) Sand Point core SPVC-2 (this study). Only the five most common species are shown (across all four cores). Note differences in depth axes. Minimum dissimilarity between each core sample and its closest modern analog provides an estimate of ecological plausibility. Samples with a minimum dissimilarity less than the 20th percentile of the modern training set are considered to have a good modern analog. Depths corresponding to ~750 CE and ~1450 CE (times encompassing possible reorganizations of the Outer Banks) are shown for reference. Clusters were identified using stratigraphically-constrained cluster analysis. Summary descriptions of core sediment are presented.

processing. Although the full core was collected (from the surface downward), only the interval below 0.80 m was analyzed because our intention was to overlap with and extend the existing record

from Tump Point (~1.20-m long), rather than to produce a reconstruction that extended to the present. This depth cut-off for analysis was based on an initial assumption that Hill Point and

Tump Point shared a RSL history (and rate of sediment accumulation) given their proximity to one another. The choice of 0.80 m reflects the practical convenience of restricting our analysis to specific, 0.5-m long sections of the core as they were collected in the field (i.e., 0.80–1.30 m onwards). It does not represent a stratigraphic boundary and was used as a guide during analysis rather than as a fixed and immovable threshold. Core-top elevations were measured using real time kinematic satellite navigation, where a base station established the elevation of a temporary benchmark (using the GEOID 12 model with a reported root mean square error of 0.012 m) and elevations relative to that benchmark were measured using a total station. Conversion of measured elevations from North American Vertical Datum of 1988 (NAVD88) to local tidal datums was achieved using the Vdatum transformation tool (Hess et al., 2005).

In Croatan Sound adjacent to the Sand Point salt-marsh platform, divers previously observed organic-rich sediment on the bottom of the sound and we used a Chirp seismic survey to identify locations that were likely to preserve thick accumulations of salt-marsh peat. We collected five vibracores (SPVC-1 to SPVC-5; Fig. 1C) in shallow (less than 3.5-m deep) water from the East Carolina University RV *Stanley R. Riggs*. Each core was collected by vibrating an 8-cm diameter aluminum irrigation pipe into the sediment. The soft nature of the sediment meant that minimal resistance was encountered during coring. Divers deployed in the water ensured that each pipe was vertical throughout collection. When each core was ended in resistant sediment, we measured the distance between the top of the core and the sediment surface on the inside and outside of the pipe to estimate how much compaction (shortening) occurred during coring. The cores were extracted using a shipboard A-frame. We selected SPVC-2 for detailed analysis because it included a thick, unbroken sequence of high salt-marsh peat with abundant remains of *Juncus roemerianus* and underwent no measurable compaction during coring. SPVC-2 is located ~550 m from the Sand Point core collected and analyzed by Kemp et al. (2011; Fig. 1C). The core was capped and labeled in the field before being cut to 1-m long sections, split for transportation, wrapped in plastic and refrigerated. We established a temporary benchmark on the Sand Point salt marsh using real time kinematic satellite navigation (base station only with the GEOID12 model). The reported root mean square uncertainty of this measurement was 0.012 m. The elevation of each core top (i.e., the sediment surface beneath Croatan Sound at the location of the core) was then tied to the temporary benchmark using a total station. Due to the relatively shallow nature of Croatan Sound and the cores that we collected, some of the vibracore pipe remained exposed above the surface of the water upon completion of coring. This enabled a reflector to be accurately and stably placed on the top of the core pipe for leveling. The depth from the top of the pipe to the sediment surface (i.e. the core top) was recorded by the divers using a tape measure. We used Vdatum (Hess et al., 2005) to convert from NAVD88 to local tidal datums.

### 3.2. Microfossil analysis and paleomorph elevation

We enumerated foraminifera from 0.01-m thick samples (approximately 1 cm<sup>3</sup> volume) in HP-9 (Kegel, 2015) and SPVC-2 that were sieved under running water to retain material in the 63–500 μm size fraction. Foraminifera were counted in water under a binocular microscope and identified with reference to type slides held in the Cushman Collection at the Smithsonian Institution (Washington D.C.), The Natural History Museum (London) and literature pertaining to salt-marsh foraminifera in the study region (e.g., Culver and Horton, 2005; Horton and Culver, 2008; Kemp et al., 2009b; Robinson and McBride, 2006; Vance et al., 2006;

Wright et al., 2011). We counted a minimum of 100 foraminiferal tests in each sample unless fewer were present, in which case the entire sample was counted. This count size and approach is appropriate for the low-diversity assemblages that are typical of salt-marsh foraminifera (e.g., Fátela and Taborda, 2002) and which frequently display variability in concentration (number of tests per unit volume of sediment) that can reach an order of magnitude even in adjacent (or replicate) modern samples collected from the same environment (e.g., Hawkes et al., 2010; Horton and Edwards, 2006). Therefore we did not use the concentration of foraminifera to draw inferences about paleoenvironmental conditions. Counts of foraminifera from the Tump Point and Sand Point cores were unchanged from those presented in Kemp et al. (2011). To establish the depositional environment in the lowermost part of HP-9, we prepared ten samples for pollen analysis following standard methods (Traverse, 2007) and counted a minimum of 300 pollen grains and fern spores.

Paleomorph elevation (PME) is the elevation with respect to a contemporary tidal datum at which a core sample originally accumulated. It is estimated based on the analogy between foraminifera in the core and their counterparts observed in analogous modern environments. PME can be reconstructed (with uncertainty) using transfer functions, which are numerical techniques that quantify the relationship between foraminifera and tidal elevation using empirical data (e.g., Juggins and Birks, 2012). Kemp et al. (2011) used this approach to reconstruct RSL at Tump Point and Sand Point. Although the 1σ uncertainty of these reconstructions was small (approximately ± 0.03–0.06 m), it was large compared to the great diurnal tidal range (~0.12 m). Barlow et al. (2013) summarized the results from several published transfer functions for reconstructing PME and showed that sites with smaller tidal ranges had correspondingly small uncertainties that were large relative to tidal range. On this basis Kemp et al. (2014) contended that the usefulness of transfer functions over classification methods was diminished at sites with small (less than ~1 m) tidal ranges. In the specific case of North Carolina where tidal ranges in back-barrier estuaries are small (less than 0.2 m), PME estimates generated by assigning core samples to either a “low” or “high” salt-marsh group on the basis of foraminiferal content have comparable, or better, precision to those from a transfer function (Kemp et al., 2009a, 2009c; Fig. S1). Therefore, we reconstruct PME using a binary classification where low and high salt-marsh assemblages are recognized by their compositional similarity to modern equivalents in the regional-scale training set with consideration of sediment texture (e.g., Kemp et al., 2009b). Low salt-marsh assemblages are recognized by high abundances of *Miliammina fusca* and/or *Ammobaculites* spp. and form between MTL and mean high water (MHW) in an environment characterized by the deposition of organic silt and clay. At Tump Point and Hill Point this range is equivalent to 0.06 m MTL ± 0.06 m, compared to 0.08 m MTL ± 0.08 m at Sand Point. High salt-marsh assemblages are distinguished by high abundances of one or more of *Haplophragmoides wilberti*, *Trochammina inflata*, *Arenoparrella mexicana*, *Jadammina macrescens* and *Tiphrotrocha comprimata*. These assemblages form between MHW and the highest occurrence of foraminifera (Wright et al., 2011) and are associated with sediment that is comprised of salt-marsh peat. This range corresponds to 0.24 m MTL ± 0.12 m at Tump Point and Hill Point compared to 0.31 m MTL ± 0.16 m at Sand Point. We treat these ranges as a normally-distributed 2σ uncertainty. The range for the high salt-marsh assemblage is likely a conservative estimate because wind-driven water levels elevate the lower limit of peat-forming vegetation communities that support assemblages of foraminifera. To ensure comparability among reconstructions, we reassigned PMEs to samples in the existing Tump Point and Sand Point cores using this

approach. A comparison of classification and transfer-function based approaches to estimating PME is presented and discussed in the supplementary materials (Fig. S1).

The ecological plausibility of PME reconstructions was assessed using the measured dissimilarity (Bray-Curtis distance metric) between each core sample and its closest modern analog in the modern training set. It remains important to test the degree of analogy between modern and core assemblages even when PME is estimated by classification. Samples with a minimum dissimilarity greater than the 20th percentile of distances measured among all possible pairs of modern samples were judged to lack a modern analog and were excluded from the resulting RSL reconstruction (e.g., Jackson and Williams, 2004; Overpeck et al., 1985; Watcham et al., 2013). We identified significant changes in foraminiferal assemblages within each core using stratigraphically-constrained cluster analysis (Grimm, 1987), where the number of groups was determined from a broken stick plot. Microfossil data from the four cores are tabulated in the supporting appendix.

### 3.3. Radiocarbon dating and the development of age-depth models

Identifiable plant macrofossils in HP-9 and SPVC-2 were isolated from the sediment matrix to provide a suite of potential samples for radiocarbon dating. We dated macrofossils that grew, or were deposited on (or close to) paleomarine surfaces (e.g., rhizomes of common salt-marsh plants and wood fragments) with an approximately even distribution throughout each core (Table 1). Identification of macrofossils was based on comparison to modern examples collected in the field and by reference to published descriptions and illustrations (e.g., Eleuterius, 1976b, 2000; Kemp et al., 2013b; Niering et al., 1977). Each sample was cleaned under a microscope to remove contaminating material, dried at ~40 °C, and submitted to the National Ocean Sciences Accelerator Mass Spectrometry (NOSAMS) facility for dating. All samples underwent standard acid-base-acid pretreatment, conversion to graphite and  $\delta^{13}\text{C}$  was measured on an aliquot of  $\text{CO}_2$  gas collected during sample

combustion.

A Bchron age-depth model was developed for HP-9 and SPVC-2 using the depth of the reported radiocarbon ages in each core as an input (Haslett and Parnell, 2008; Parnell et al., 2008, 2011). As part of this procedure the radiocarbon ages were calibrated using the IntCal13 dataset (Reimer et al., 2013). For each 0.01-m thick interval of the cores, Bchron generated posterior age estimates using Markov Chain Monte Carlo simulation. Each of the resulting sediment accumulation histories has equal probability and the resulting suite of chronologies is used to produce a 95% credible interval for sample age (for all reported ages the accompanying uncertainty is the 95% credible interval).

To ensure comparability among RSL reconstructions, we generated a revised age-depth model for the Tump Point and Sand Point cores of Kemp et al. (2011) using the same version and configuration of Bchron as was applied to HP-9 and SPVC-2. These revised age-depth models included age estimates from sources other than radiocarbon dating and two additional radiocarbon dates for Tump Point. Bomb spike radiocarbon dates were calibrated using the Northern Hemisphere zone 2 dataset (CaliBomb software; Reimer et al., 2004) prior to inclusion in the age-depth model and the calibrated ages were treated as having a normal probability distribution. The maximum downcore activity of  $^{137}\text{Cs}$  was assigned an age of  $1963 \pm 1$  CE (e.g., Delaune et al., 1978; Turekian et al., 1980) and was included in the age-depth model with a normal probability distribution. In the Sand Point core, we interpreted the increased abundance of *Ambrosia* pollen as evidence of land clearance by Europeans (e.g., Brugam, 1978; McAndrews, 1988) and assigned this depth an age of  $1720 \text{ CE} \pm 20$  years (Cooper et al., 2004) with a normal probability distribution. The results from  $^{210}\text{Pb}$  dating were excluded from the reanalysis because accumulation rates modeled from  $^{210}\text{Pb}$  measurements are used to assign ages (with uncertainty) to multiple depths in a core (Appleby and Oldfield, 1992). While this technique is an accurate and precise means to estimate age in cores of salt-marsh sediment (e.g., Anisfeld et al., 1999; Sharma et al., 1987), the suite of age-

**Table 1**  
Reported radiocarbon ages.

Core	Depth in Core (m)	Sample ID	Reported $^{14}\text{C}$ Age and Error	$\delta^{13}\text{C}$ (‰, PDB)	Description
HP-9	0.88	OS-107656	$625 \pm 30$	-27.19	<i>Juncus roemerianus</i> stem
HP-9	0.98	OS-107657	$680 \pm 25$	-26.66	<i>Juncus roemerianus</i> stem and rhizome bulb
HP-9	1.10	OS-107658	$975 \pm 30$	-27.39	<i>Juncus roemerianus</i> stem
HP-9	1.24	OS-110628	$1180 \pm 25$	-24.53	<i>Juncus roemerianus</i> stem
HP-9	1.39	OS-107659	$1440 \pm 25$	-27.55	<i>Juncus roemerianus</i> rhizome
HP-9	1.53	OS-107661	$1500 \pm 20$	-28.22	<i>Juncus roemerianus</i> rhizome
HP-9	1.77	OS-107663	$1880 \pm 25$	-14.50	<i>Distichlis spicata</i> rhizome
HP-9	1.93	OS-120937	$1990 \pm 25$	-27.07	<i>Juncus roemerianus</i> stem and rhizome bulb
HP-9	2.06	OS-107768	$2180 \pm 25$	-28.77	<i>Juncus roemerianus</i> stem and rhizome bulb
HP-9	2.10	OS-120938	$2170 \pm 20$	-28.91	<i>Juncus roemerianus</i> stem and rhizome bulb
HP-9	2.16	OS-122234	$2550 \pm 20$	-27.39	<i>Juncus roemerianus</i> stem
HP-9	2.26	OS-122233	$2610 \pm 15$	-27.06	<i>Juncus roemerianus</i> stem
HP-9	2.46	OS-107785	$3480 \pm 25$	-26.30	Piece of wood
HP-9	2.67	OS-107786	$5000 \pm 35$	-26.54	<i>Schoenoplectus</i> spp. stems
SPVC-2	0.14	OS-110634	$1650 \pm 25$	-28.23	<i>Juncus roemerianus</i> stem
SPVC-2	0.29	OS-115117	$1840 \pm 20$	-27.12	<i>Juncus roemerianus</i> stem
SPVC-2	0.37	OS-117595	$1960 \pm 20$	-27.13	<i>Juncus roemerianus</i> stem
SPVC-2	0.46	OS-115118	$2110 \pm 20$	-28.1	<i>Juncus roemerianus</i> stem
SPVC-2	0.54	OS-117596	$2150 \pm 20$	-27.36	<i>Juncus roemerianus</i> stem
SPVC-2	0.65	OS-110635	$2230 \pm 25$	-15.23	<i>Distichlis spicata</i> rhizome
SPVC-2	0.74	OS-117597	$2470 \pm 25$	-26.34	<i>Juncus roemerianus</i> stem
SPVC-2	0.83	OS-115119	$2530 \pm 20$	-13.94	<i>Distichlis spicata</i> rhizome
SPVC-2	0.93	OS-115120	$2490 \pm 25$	-25.20	Woody stem and rhizome bulb
SPVC-2	1.04	OS-110636	$2780 \pm 40$	-28.16	<i>Juncus roemerianus</i> stem
SPVC-2	1.17	OS-115121	$2880 \pm 20$	-26.66	Fibrous plant stem and bulb
SPVC-2	1.44	OS-110637	$3320 \pm 35$	-27.92	<i>Juncus roemerianus</i> stem

Radiocarbon ages reported by the National Ocean Sciences Accelerator Mass Spectrometry facility for macrofossils in Hill Point core 9 (HP-9) and Sand Point vibracore 2 (SPVC-2). Ages and errors following the rounding conventions of (Stuiver and Polach, 1977). Sample  $\delta^{13}\text{C}$  values are relative to the Pee Dee Belemnite (PDB) standard.

depth estimates that it produces are not independent of one another, which invalidates an assumption of the Bchron age-depth model. Including age estimates from  $^{210}\text{Pb}$  measurements would therefore unfairly bias the age-depth model toward the large number of coherent data points produced from a single chronological technique (De Vleeschouwer and Parnell, 2014; Kemp et al., 2013a). Alternatively, age estimates from  $^{210}\text{Pb}$  could be down weighted in an age-depth model so that when combined with other chronological information they have the same weight as a single data point such as an individual radiocarbon age. Reported radiocarbon ages are presented in Table 1. Sample ages estimated by the four age-depth models are tabulated in the supporting appendix.

#### 3.4. Reconstructing relative sea level

We reconstructed RSL using the following equation:

$$\text{RSL}_i = \text{Sample Altitude}_i - \text{PME}_i \quad (1)$$

Where the altitude of sample  $i$  was measured directly (depth below core top of known elevation) and paleomorph elevation ( $\text{PME}_i$ ) was estimated using foraminifera preserved in the corresponding sample. The age of each sample was estimated using the Bchron age-depth model. In cores where all samples have the same PME, the resulting RSL reconstruction is a function of the accumulation history represented by the age-depth model. RSL trends were quantified by applying the Error-In-Variables Integrated Gaussian Process (EIV-IGP) model of Cahill et al. (2015). This approach quantitatively takes into consideration the sample-specific nature of age and vertical uncertainties (with their associated probability distributions) for individual data points and their uneven distribution through time. These models display edge effects, where uncertainty at the start and end of the records gets larger. Parameters in the EIV-IGP model were estimated from the datasets using the priors that are specified and described in Cahill et al. (2015). Rates of RSL change estimated using the EIV-IGP model are reported as a mean and uncertainty representing a 95% credible interval and rounded to one decimal place. RSL reconstructions from each of the four cores are tabulated in the supporting appendix.

## 4. Results

### 4.1. Microfossils and paleomorph elevation

Assemblages of foraminifera in the Tump Point core were described by Kemp et al. (2011) and are unaltered in this study (Fig. 2A). Foraminifera were sparse or absent at depths below 1.40 m. In the upper 1.40 m of the core, we identified four assemblages using stratigraphically-constrained cluster analysis. The most abundant species between 1.40 m and 0.72 m (cluster 4) were *H. wilberti*, *T. inflata* and *A. mexicana*. Three samples at 0.69–0.66 m were dominated by *A. mexicana* (cluster 3). The interval from 0.64 m to 0.24 m (cluster 2) is dominated by *H. wilberti*, while the uppermost 0.24 m of the core (cluster 1) is characterized by the high abundance of *A. mexicana*. The measured dissimilarity between all core samples and their closest modern analog was less than the 20th percentile of dissimilarity measured in all possible pairings of modern samples and we therefore retained all core samples for reconstructing RSL. All core samples were classified as having formed in a high salt-marsh environment and assigned a PME of 0.24 m MTL  $\pm$  0.12 m.

The new core from Hill Point (HP-9) was composed of a light-brown basal sand unit at depths below 2.76 m. We interpret this unit to be an incompressible, pre-Holocene substrate. This is overlain by a black, amorphous organic unit (2.76–1.39 m) in which

some sand is present below ~2.15 m. The presence of sand may indicate vertical mixing from the underlying unit, intermittent marine incursions and/or transportation from a nearby source of sand through other mechanisms such as wind. The uppermost 1.39 m is a dark brown, high salt-marsh peat with abundant plant macrofossils (primarily *J. roemerianus*). The contact between this unit and the underlying amorphous organic unit is diffuse and the quantity and preservation of plant macrofossils increases up core. The core top elevation was 0.14 m MTL. Foraminifera were only enumerated from samples at depths below 0.80 m (Fig. 2B). Below 2.30 m, foraminifera were sparse or absent and pollen analysis performed on samples between 2.71 m and 2.28 m (Fig. 3) qualitatively indicates that the Hill Point site was likely a supra-tidal wetland as evidenced, for example, by high abundances of Poaceae and Asteraceae. The lowest occurrence of foraminifera is in the unit of black, amorphous organic sediment, which is common for transgressive successions on the U.S. Atlantic coast because foraminifera respond more rapidly to changes in tidal inundation than plant communities and bulk-sediment characteristics such as organic content (e.g., Kemp et al., 2012). For example, Craft et al. (2002) estimated that salt-marsh plants in North Carolina could colonize a freshwater upland in response to RSL rise in 3–5 years, but that it could take 200 years for this succession to be recognizable in bulk sediment. Furthermore, there is often little difference in the texture and color of sediment deposited in supra-tidal wetlands and the neighboring highest salt-marsh environments. Stratigraphically-constrained cluster analysis identified five distinct assemblages of foraminifera. Between 2.30 m and 1.80 m, the most common species of foraminifera was *A. mexicana* (cluster 5). Clusters 4 (1.76–1.69 m) and 3 (1.67–1.60 m) have elevated, but varying abundances of *J. macrescens*. At 1.56–1.10 m, the core was characterized by *T. comprimata* (cluster 2) and the interval from 1.06 m to 0.80 m was distinguished by increased abundance of *A. mexicana* (cluster 1). All core samples had a minimum measured dissimilarity less than the 20th percentile threshold and were therefore retained in the RSL reconstruction. All samples were dominated by high salt-marsh species of foraminifera and assigned a PME of 0.24 m MTL  $\pm$  0.12 m.

Foraminifera in the Sand Point Russian core from Kemp et al. (2011) are utilized in this study (Fig. 2C). Foraminifera were sparse or absent below 2.68 m and stratigraphically-constrained cluster analysis identified three assemblages. The dominant species were *J. macrescens* with *H. wilberti* between 2.68 m and 1.50 m (cluster 3). The interval from 1.47 m to 0.33 m was characterized by

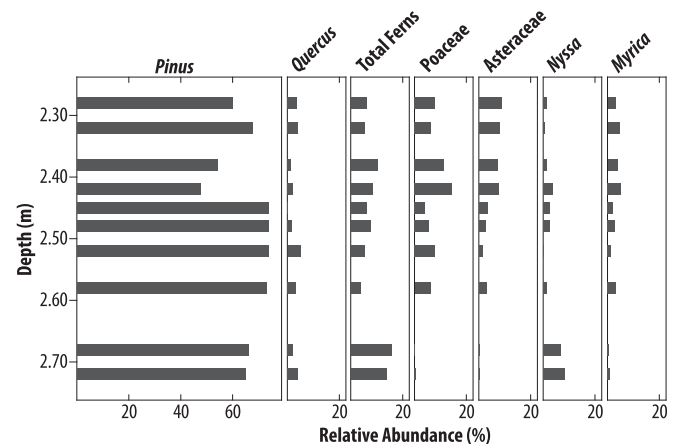


Fig. 3. Pollen content of samples in Hill Point core HP-9 at depths from 2.28 to 2.72 m. These assemblages and the absence of foraminifera indicate that the site was a forested and freshwater wetland at the time of sediment deposition.

a near mono-specific assemblage of *J. macrescens* (cluster 2), while *H. wilberti* became dominant from 0.32 m to 0.17 m (cluster 1). All samples in the core had modern analogs as evidenced by minimum dissimilarities less than the 20th percentile threshold and were classified as having formed in a high salt-marsh environment. Consequently, these samples were assigned a PME of 0.31 m MTL  $\pm$  0.16 m.

Core SPVC-2 (Fig. 2D) included a basal unit of consolidated clay and silt at depths from 2.60 m to at least 4.28 m (end of core). This was overlain at 2.60–1.95 m by grey silt with occasional, but unidentified, plant remains. Between 1.95 m and 1.42 m, the sediment was a mottled grey-brown peat with identifiable remains of *J. roemerianus* and lower organic content at greater depths. A unit of black, amorphous peat was present at 1.42 m–1.12 m and the uppermost 1.12 m of the core was comprised of a brown high salt-marsh peat with abundant *J. roemerianus* macrofossils. The core top elevation was 1.78 m below MTL. Foraminifera were sparse or absent below 1.20 m (Fig. 2D). From 1.20 m to 0.73 m, the dominant species of foraminifera were *J. macrescens* with *T. comprimata* (cluster 2). Above 0.73 m, the abundance of *T. comprimata* decreased and *J. macrescens* remained dominant (cluster 1). All core samples had modern analogs and were classified as having formed in a high salt-marsh environment. Consequently, these samples were assigned a PME of 0.31 m MTL  $\pm$  0.16 m.

#### 4.2. Chronology and age-depth models

The Tump Point core spans the period since ~400 CE (1.50 m) and the earliest occurrence of foraminifera occurs at ~550 CE (Fig. 4A). The average uncertainty for estimated sample age was  $\pm$ 54 years. The smallest sample-specific uncertainty was  $\pm$ 4 years close to the top of the core where a concentration of bomb-spike radiocarbon dates and the presence of a  $^{137}\text{Cs}$  spike provide tight constraints for the Bchron model.

The history of sediment accumulation at Hill Point was constrained by 14 radiocarbon dates at depths between 0.80 m and 2.67 m (Table 1, Fig. 4B). The resulting Bchron age-depth model shows that the interval from 2.67 m to ~2.30 m was deposited slowly from approximately 4000 BCE to 1000 BCE. Pollen evidence (coupled with the absence of foraminifera and sediment texture) qualitatively indicates that this sediment accumulated in a freshwater wetland environment at elevations above regular tidal inundation (Fig. 3). After ~1000 BCE the rate of accumulation increased significantly at a time coincident with the first occurrence of foraminifera. For samples with counts of foraminifera, the average uncertainty in sample age was  $\pm$  100 years, but varied from  $\pm$  31 years to  $\pm$  318 years. The largest errors occur near the highest dated level and near the change in accumulation rate at ~2.30 m. The increased uncertainty close to the highest dated level arises as a predictable edge effect because of the way in which Bchron utilizes and shares information among samples (Parnell and Gehrels, 2015; Parnell et al., 2008).

Reanalysis of the chronology for the Sand Point Russian core shows that the core spans the period from approximately 600 BCE to 1975 CE and that foraminifera are present from ~200 BCE onwards (Fig. 4C). The average uncertainty for samples with counts of foraminifera was  $\pm$  47 years, with the smallest errors being predicted for samples near to the top of the core where a high density of age estimates from  $^{137}\text{Cs}$  and bomb-spike radiocarbon dates provides a tight control on the history of sediment accumulation.

Twelve radiocarbon dates from SPVC-2 show that sediment from 1.40 m to the top of the core (which is the sediment surface at the bottom of Croatan Sound) accumulated between ~1600 BCE and ~600 CE (Fig. 4D). We conclude that erosion of the Roanoke Marshes removed the salt-marsh sediment that likely formed at the

core site between ~600 CE (core-top age) and ~1800 CE, when the site transitioned from a depositional to an erosive environment (e.g., Riggs and Ames, 2003; Riggs et al., 2000). Foraminifera were present in samples deposited after ~1150 BCE and the average uncertainty for estimated sample age was  $\pm$  72 years.

#### 4.3. Relative sea level

The Tump Point reconstruction demonstrates that RSL rose by ~1.5 m since ~600 CE, while RSL at Hill Point rose from approximately -2.4 m at ~1000 BCE to -1.1 m at ~1600 CE (Fig. 5A). These records overlap with one another and therefore we combine them into a single dataset that is taken to be representative of the late Holocene RSL history of Cedar Island (Fig. 5C). At Cedar Island, RSL rose at ~0.3 mm/yr from ~1000 BCE to 250 BCE, although this rate is uncertain due to edge effects at the beginning of the reconstruction (Fig. 6A). The rate of rise increased to ~0.9 mm/yr at ~0 CE and was sustained until the 18th century. Since ~1800 CE RSL rise accelerated continuously (but at varying rates) until reaching the current rate of  $-2.4 \pm 0.7$  mm/yr, which is consistent with nearby tide-gauge records (e.g., Kopp, 2013; Zervas, 2009) and is the fastest, century-scale rise in the late Holocene.

The Sand Point Russian core records ~2.6 m of RSL rise since ~200 BCE, while the reconstruction from SPVC-2 records a RSL rise from approximately -3.3 m at ~1200 BCE to -2.1 m at ~650 CE (Fig. 5B). The agreement between these two records justifies our decision to combine them into a single dataset that is representative of the late Holocene RSL history of Roanoke Island (Fig. 5C). At Roanoke Island, RSL rose at ~0.7 mm/yr from ~1100 BCE to ~600 CE, before accelerating to achieve a peak rate of rise ( $1.5 \pm 0.1$  mm/yr) at ~1100 CE (Fig. 6B). The rate of rise then declined to  $1.1 \pm 0.1$  mm/yr at ~1550 CE, since when RSL rise accelerated continuously (but at varying rates) to reach a current rate of  $-2.2 \pm 0.9$  mm/yr, which is consistent with nearby tide-gauge records (e.g., Kopp, 2013; Zervas, 2009) and is the fastest, century-scale rise in the late Holocene.

## 5. Discussion

### 5.1. Differences between Cedar Island and Roanoke Island

A key conclusion of the Kemp et al. (2011) North Carolina RSL reconstructions was that Tump Point and Sand Point recorded the same sea-level changes after correction for GIA (and other processes causing spatially-variable vertical land motion). Caveats to this conclusion included the limited period of time (~1100–1975 CE) for which RSL reconstructions existed at both sites and the large chronological uncertainty in the earliest part of the Tump Point record. In this study, we estimated the difference (with uncertainty) between RSL at Cedar Island and Roanoke Island using the EIV-IGP model because the distribution of data points through time is not the same in both records. This analysis shows an overall decrease in the RSL difference between sites, from ~0.8 m at ~1000 BCE to zero at present (Fig. 5D) in general agreement with Earth-ice models (e.g., ICE6G-VM5; Roy and Peltier, 2015) that predict RSL rise at Roanoke Island to be 0.1–0.2 mm/yr faster than at Cedar Island (Fig. 5D). The RSL difference decreases non-linearly, however, and is interrupted by an interval (~0 CE to 600 CE) during which a near constant 0.5 m difference is maintained, after which the difference rapidly declines to 0.1 m or less by ~1400 CE (Fig. 5D). At 600–1100 CE this pattern is strongly influenced by acceleration in the rate of RSL rise at Roanoke Island (and specifically the Sand Point Russian core) from ~0.8 mm/yr to a peak of 1.5 mm/yr (95% credible interval of 1.3–1.6 mm/yr). Subsequently, the rate of RSL rise at Roanoke Island decelerated to ~1.0 mm/yr at ~1400 CE (Fig. 6B and C). This feature is absent in the Cedar Island

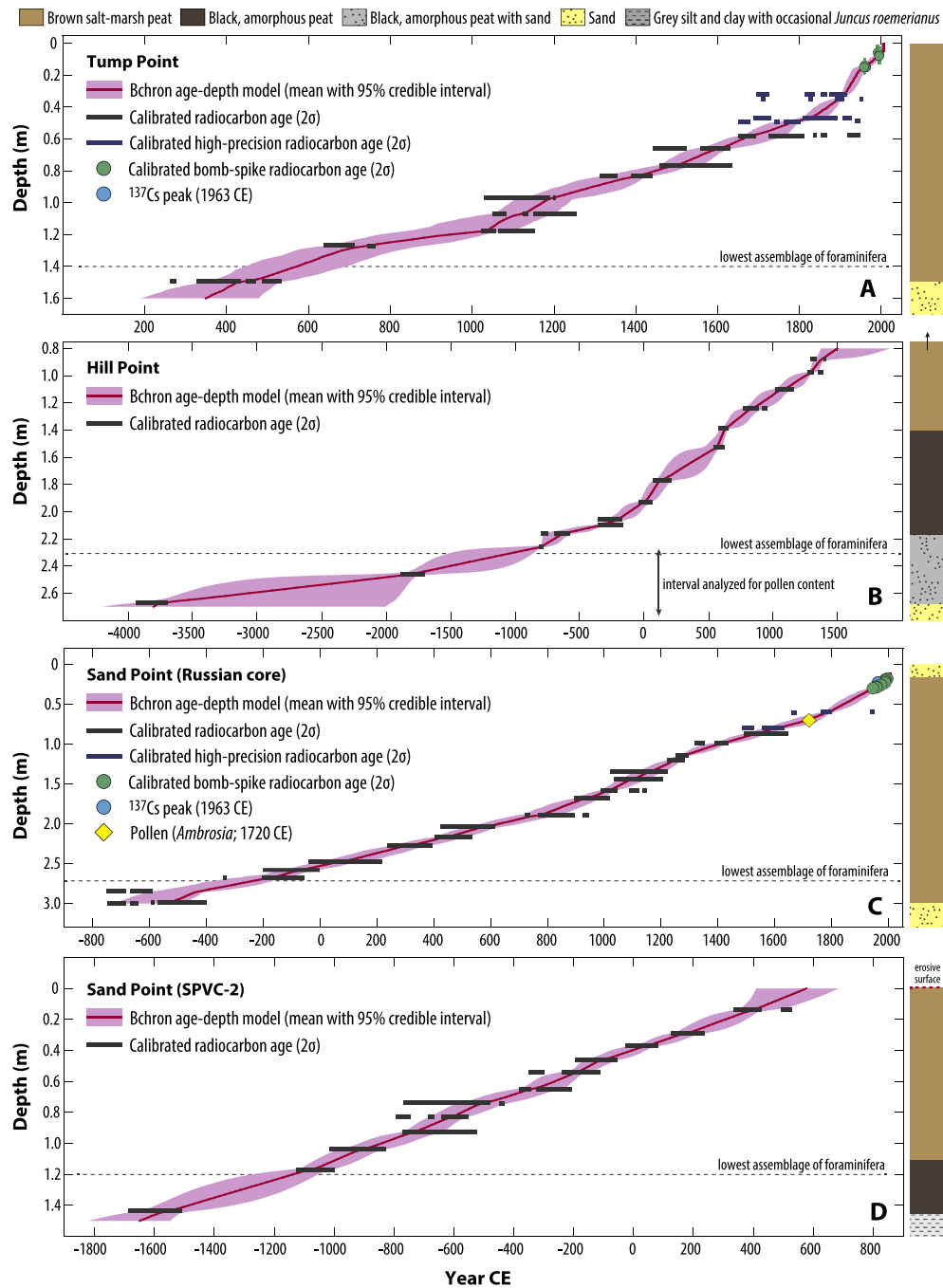


**Fig. 4.** Age-depth models generated using Bchron for cores of salt-marsh sediment from (A) Tump Point (Kemp et al., 2011), (B) Hill Point (HP-9; this study), (C) Sand Point Russian core (Kemp et al., 2011), and (D) Sand Point vibracore (SPVC-2; this study).

reconstruction, which shows a consistent RSL rise of  $\sim 0.7$  mm/yr for the same period (Fig. 6A). Below, we explore if and how contributions from GIA (and other sources of vertical land motion), local-scale processes (sediment compaction, sediment dynamics and tidal-range change) and ocean/atmosphere dynamics may have caused the reconstructed RSL differences between Cedar Island and Roanoke Island.

### 5.2. Glacio-isostatic adjustment and vertical land motion

Along the passive margin of the North American Atlantic coast, ongoing and spatially-variable GIA was a primary driver of

regional-scale, late Holocene RSL trends (e.g., Davis and Mitrovica, 1996; Engelhart et al., 2009; Peltier, 1996). Kemp et al. (2011) detrended the RSL reconstructions for Sand Point and Tump Point by rates of 1.0 mm/yr and 0.9 mm/yr respectively that were assumed to represent contributions from processes that could be treated as linear over the past  $\sim 2000$  years, namely GIA, but also tectonic motion arising from spatial differences in the geological structures underlying coastal North Carolina (e.g., Riggs, 2002; Riggs and Ames, 2003; van de Plassche et al., 2014). GIA predictions generated using common Earth-ice models (ICE5G-VM2 and ICE6G-VM5) confirm that RSL rise during the past  $\sim 2000$  years was 0.1–0.2 mm/yr faster at Roanoke Island than at Cedar Island

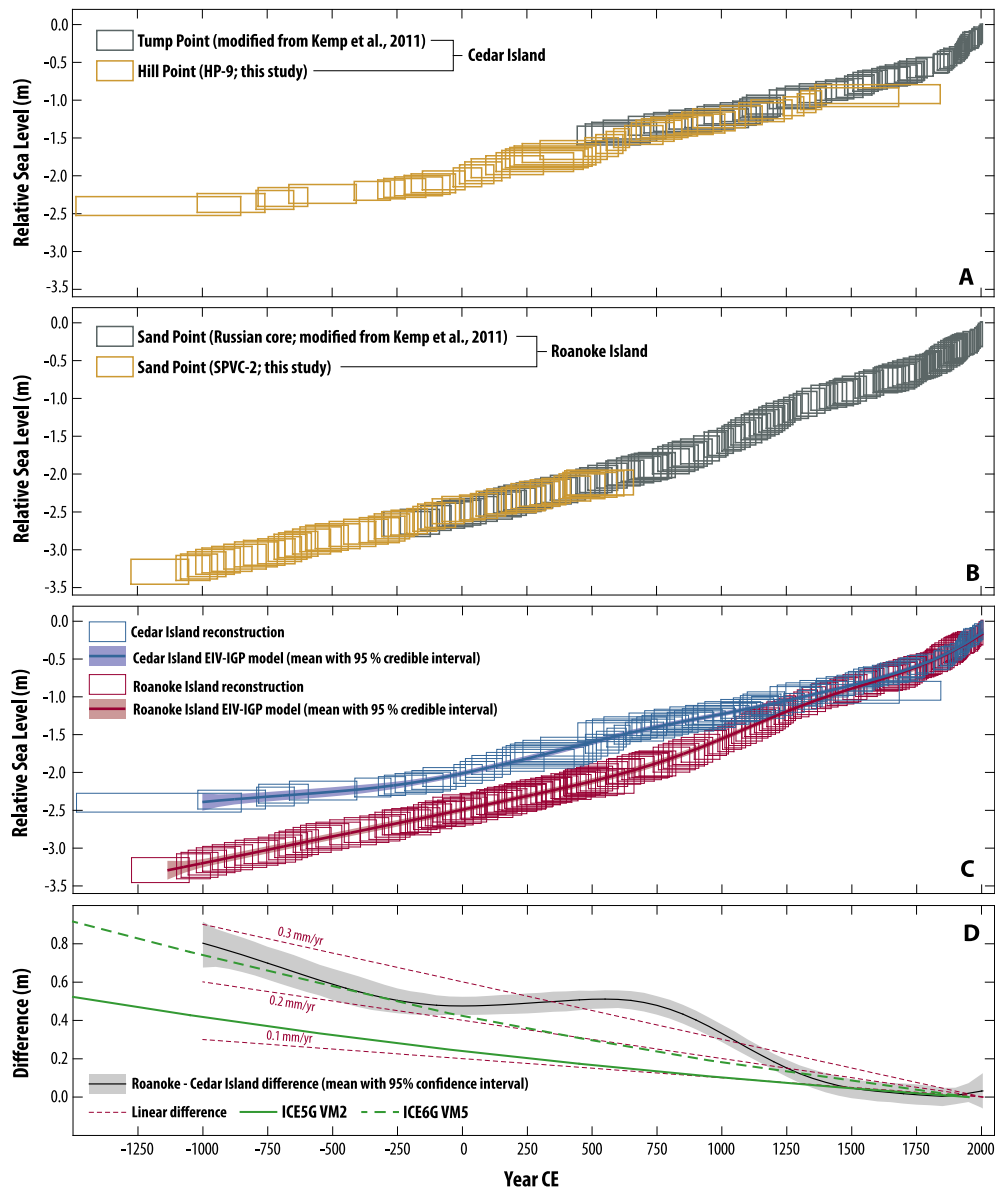


**Fig. 5.** Relative sea level (RSL) reconstructions from (A) Tump Point and Hill Point and (B) Sand Point. Boxes represent the  $2\sigma$  vertical and chronological uncertainty. Vertical uncertainty arises from classification of foraminiferal assemblages as being deposited in a high salt-marsh environment between mean high water and the highest occurrence of foraminifera in the regional-scale modern training set. The chronological uncertainty is from the Bchron age-depth model developed for each core. (C) The Tump Point and Hill Point reconstructions were combined to produce the single record that is representative of RSL trends at Cedar Island. The two Sand Point reconstructions were combined to produce the single record that is representative of RSL trends at Roanoke Island. Application of the Errors-In-Variates Integrated Gaussian Process (EIV-IGP) to the Cedar Island and Roanoke Island records provided a continuous RSL history for each region. (D) Difference between RSL at Roanoke Island and Cedar Island calculated using the EIV-IGP model. Red lines mark linear differences of 0.1, 0.2, and 0.3 mm/yr. Green lines show the difference predicted by two commonly-used Earth-ice models (Argus et al., 2014; Peltier, 2004).

(Fig. 5D). For example, the ICE5G-VM2 model estimated a linear rate of GIA-driven RSL rise of 1.05 mm/yr at Roanoke Island, compared to 0.93 mm/yr at Cedar Island over this time period (Fig. 5). Spatial differences in RSL predicted by Earth-ice models show that GIA cannot fully reconcile the observed difference between Roanoke Island and Cedar Island (Fig. 5D). From ~1000 BCE to ~0 CE the observed difference decreased from ~0.8 m to ~0.5 m, which is in good agreement with predictions from the ICE6G-VM5 model. From ~1250 CE onwards the observed difference is also in agreement with predictions from Earth-ice models. However, the observed difference from ~0 to ~1250 CE cannot be explained by spatially-variable GIA, which produces a near-linear difference between sites on decadal to millennial timescales during the late Holocene. Additional physical mechanisms are, therefore,

necessary to explain the reconstructed spatial and temporal pattern of RSL change. These processes must produce differences in RSL on spatial scales of 10s–100s of kilometers and on centennial time-scales. We explore the viability of several such processes below.

### 5.3. Sediment compaction and sediment dynamics

Compaction causes post-depositional lowering of the sediment used to reconstruct RSL and subsequently results in overestimation of the amount and rate of RSL rise (e.g., Bloom, 1964; Kaye and Barghoorn, 1964). Application of an empirical compaction model to the Tump Point core demonstrated that compaction was minimal and did not distort reconstructed RSL trends in North Carolina (Brain et al., 2015), although the model was calibrated using

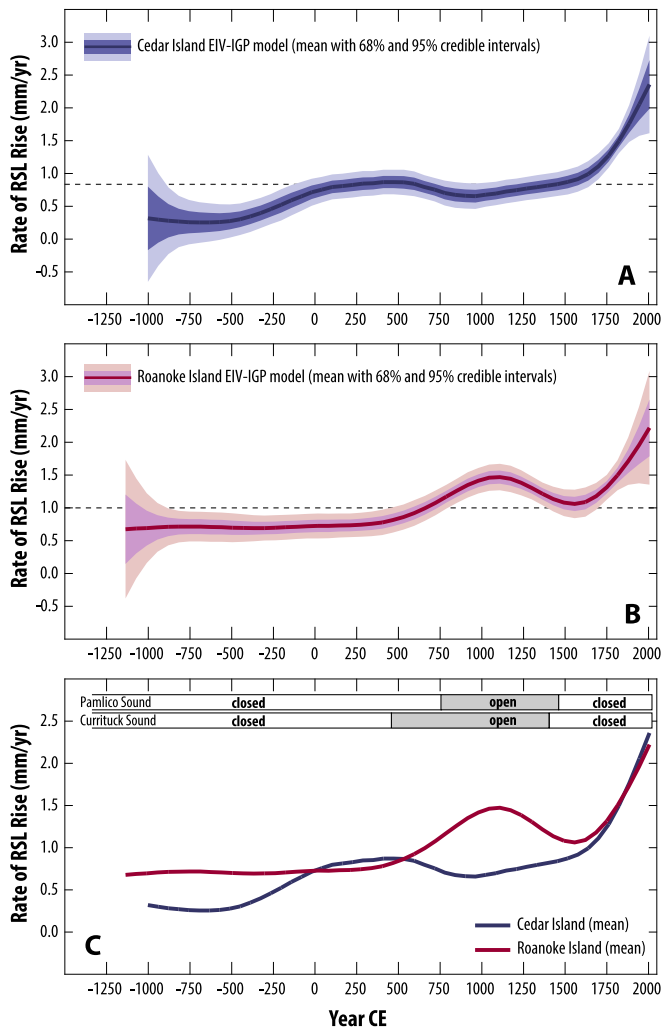


**Fig. 6.** Rates of relative sea-level (RSL) rise estimated using the Errors-In-Variables Integrated Gaussian Process (EIV-IGP) model of Cahill et al. (2015) for (A) Cedar Island and (B) Roanoke Island. Shading depicts the 68% and 95% credible intervals of the estimated rates. (C) Comparison of the mean rate of RSL rise at Cedar Island and Roanoke Island. Shaded bars mark the time periods when the Outer Banks barrier islands separating Pamlico Sound (Zaremba et al., 2016) and Currituck Sound (Moran et al., 2015) from the Atlantic Ocean were “closed” (number and size of inlets similar to present) and “open” (barrier segmented by more and/or larger inlets than present).

geotechnical measurements made on modern (surface) sediment, which may not adequately reflect sediment that was deposited in the past under different climate regimes that included phases of wetter and drier conditions (e.g., Stahle et al., 1988). The observed overlap in the Tump Point and Hill Point reconstructions, agreement between the two Sand Point cores and the continuous nature of the high salt-marsh peat units further suggests that compaction did not distort the RSL reconstructions. The Hill Point and SPVC-2 cores include high salt-marsh peat deposited on top of black amorphous peat (Fig. 2). In the case of the Hill Point core, evidence from pollen (Fig. 3), coupled with the absence of foraminifera (Fig. 2), indicates that this sediment accumulated in a freshwater wetland. Since the density of high salt-marsh peat that forms in *Juncus roemerianus*-dominated environments in North Carolina has a dry density less than water (Brain et al., 2015) this overburden is unlikely to have compacted the underlying freshwater peat if it were saturated at the time of (and since) its formation. Furthermore, the similar density of freshwater and salt-marsh peats allows the two units to be treated as a uniform sediment succession (e.g.,

Hobbs, 1986), which is unlikely to experience compaction (e.g., Brain et al., 2012). Overburden of water in Croatan Sound would not compact the salt-marsh peat in SPVC-2 if hydraulic connectivity is maintained between the water column and pore water within the peat (Powrie, 2013; Punmia and Jain, 2005). We infer that sediment deposited at the site of SPVC-2 from ~600 CE to ~1800 CE was eroded. Given the site's paleogeography and location in the Roanoke Marshes we believe that the eroded sediment was likely salt-marsh peat, which would not have caused significant post-depositional lowering of deeper sediment (e.g., Brain et al., 2015). However, the nature of the eroded material cannot be known with certainty and it remains possible that the sediment preserved in SPVC-2 experienced compaction from overlying silts and clays that were deposited (for example) in a shallow sub-tidal or tidal-flat environment (Brain et al., 2012). We propose that sediment compaction did not contribute significantly to the North Carolina RSL reconstructions and is unlikely to cause the difference in RSL between Cedar Island and Roanoke Island.

Within each of the four cores, preserved assemblages of foraminifera demonstrate that all samples were deposited in a high salt-marsh environment (Fig. 2). Subsequently, PME is constant in each core and the RSL reconstruction is driven by the history of sediment accumulation. This relationship is ecologically plausible because more frequent and longer duration flooding results in faster sediment accumulation in salt marshes (e.g., Kirwan and Murray, 2008; Morris et al., 2002). Through this feedback the salt-marsh surface can maintain a near-constant elevation with respect to tidal datums. However, local-scale sediment dynamics can cause disequilibrium between sedimentation and RSL change. If sedimentation exceeds the rate of RSL rise then the salt-marsh surface moves upward in the tidal frame (emergence). Conversely, if sedimentation falls behind the rate of RSL rise then the salt marsh moves downward in the tidal frame (drowning). This disequilibrium results in a positive/negative trend in PME that (if large enough) is manifest as changes in foraminiferal assemblages. None of the four cores showed sufficiently large and/or long-lived disequilibrium to cause a switch between high and low salt-marsh assemblages of foraminifera (Fig. 2), although it is possible that more subtle changes in PME occurred as a result of localized sediment dynamics that are overlooked by the classification-based approach that we employed. However, we contend that local-scale sediment dynamics were not an important driver of the reconstructed RSL trends for three reasons. Firstly, application of a transfer function also yields near-constant PME reconstructions (see supplemental material for a fuller discussion), indicating that the classification-based approach did not mask changes. Secondly, the high degree of coherence Hill Point with Tump Point and between the two Sand Point cores indicates that sedimentation trends are spatially consistent despite differences in geomorphology (for example Hill Point occupies a protected paleo-valley, while Tump Point is an exposed platform marsh). However, it is important to recognize that although there is good agreement between cores over the duplicated time intervals, some features of the RSL records (notably the period of faster RSL rise at Roanoke Island) are present in only a single core, which makes it challenging to definitively rule out local-scale processes as the drivers of reconstructed trends. Thirdly, if the higher rate of RSL rise reconstructed at Roanoke Island over the period 600–1100 CE is an artifact of local sediment dynamics, then the magnitude of the change would be large enough (compared to tidal range) to cause a change from high to low salt-marsh foraminifera for which there is no evidence. We conclude that the effect of local sediment dynamics is small and/or short lived and is unlikely to explain the RSL difference between Cedar Island and Roanoke Island because salt-marsh sediment accumulation rates in North Carolina achieved a

long-term equilibrium with regional-scale RSL rise.

#### 5.4. Tidal-range change

Our RSL reconstructions implicitly assumed that tidal range during the late Holocene was unchanged from the observable, modern tidal regimes at Cedar Island and Roanoke Island. However, estuaries in North Carolina are prone to tidal-range change by opening/closing of inlets, or larger discontinuities, in the Outer Banks barrier islands. If past tidal range was different to that of the present (and the interpretation of foraminifera preserved in the corresponding core samples is unchanged), then reconstructed RSL can be corrected by amending the absolute value of PME in equation (1) (sample elevation is fixed and known and remains unchanged). Correction for a paleotidal range that was larger/smaller than present (open/closed Outer Banks) results in a lower/higher RSL reconstruction. When evaluating the role of non-stationary tides in North Carolina it is important to consider paleogeography. Prior to their drowning and erosion from the mid-19th century onwards, the presence of the Roanoke Marshes likely limited exchange of water between Pamlico and Albemarle Sounds (Riggs and Ames, 2003; Riggs et al., 2000, Fig. 1). If the marshes were an absolute barrier, then prior to ~1800 CE Cedar Island was influenced only by tidal-range change in Pamlico Sound, while Roanoke Island was influenced only by tidal-range change in Albemarle Sound, allowing tidal range at either site to be modified independently of the other. Alternatively, if the Roanoke Marshes were “leaky”, then both the Cedar Island and Roanoke Island sites could be influenced (to some degree) by tidal-range change in Pamlico Sound and/or Albemarle Sound.

In Pamlico Sound, Zaremba et al. (2016) used grain-size measurements in dated sediment cores to infer energy levels during the Holocene (Fig. 6C). High-energy conditions are identified by relatively coarse material indicating that waves, currents and tides were sufficiently strong to mobilize larger sediment particles. In contrast, low-energy conditions are represented by relatively fine material, which suggests that waves, currents and tides in Pamlico Sound were weak. They showed that low-energy conditions prevailed between 1350 BCE and 750 CE, which they attributed to a barrier configuration that was similar to present in the number and/or size of inlets. In contrast, the period from 750 CE to 1450 CE was characterized by higher-energy conditions assumed to reflect a more segmented and open barrier with more and/or larger inlets and discontinuities than present. This inference is supported by the presence of planktonic foraminifera of Gulf Stream origin and shelf benthic foraminifera in Pamlico Sound sediment cores at ~800 CE to 1450 CE (Culver et al., 2007; Grand Pre et al., 2011). A return to finer grained sediment and the absence of Gulf Stream and shelf foraminifera by 1450 CE is evidence for (re)closing of the barrier between Pamlico Sound and the Atlantic Ocean. Stratigraphically-constrained cluster analysis of foraminiferal assemblages in the Hill Point and Tump Point cores indicates that assemblage changes did not coincide with the proposed timing of these regional changes in the geomorphology of the Outer Banks (Fig. 2). However, qualitative changes in foraminifera such as a modest reduction in the abundance of *J. macrescens* and increased abundances of *A. mexicana* and *T. comprimata* at Hill Point from 750 to 1450 CE could reflect changing salinity in Pamlico Sound (Kemp et al., 2009b) concurrent with opening/closing of the barrier, or with wider changes in climate such as wet/dry phases that can occur independently of RSL change (e.g., Stahle et al., 1988).

We explore the potential effect of this geomorphic evolution on our Cedar Island RSL reconstruction using simple, but illustrative paleotide scenarios in which the barrier was opened instantaneously at 750 CE (in keeping with a proposed mechanism of

barrier segmentation caused by high-energy events; e.g., one or more major hurricane landfalls) and remained open until 1100 CE, after which it reclosed gradually and by 1450 CE had achieved the same configuration as it began with in 750 CE (Fig. 7A). If opening the barrier doubled tidal range at Cedar Island (compared to 0.13 m today), then the corrected RSL reconstruction is lowered by up to 0.16 m (Fig. 7B) and the rate of RSL rise is correspondingly lower than the original reconstruction from ~400 CE to ~1000 CE (minimum of ~0.3 mm/yr at 750 CE), followed by elevated rates of RSL rise from ~1000 CE to ~1750 CE (Fig. 7C). This pattern is maintained, but exaggerated, in a scenario where tidal range is increased by a factor of five. If the Roanoke Marshes prevented exchange of water between Pamlico and Albemarle Sounds, then increased tidal range at Cedar Island caused by opening of the barrier results in a corrected RSL curve that is less similar to Roanoke Island than the original reconstruction with stationary tides. This is illustrated by the calculated RSL difference between Cedar Island and Roanoke Island compared to the difference under assumed stationary tides (Fig. 7F). Within the geomorphic constraint, to produce a faster rate of rise at Cedar Island that is in better agreement with the Roanoke Island, tidal range would need to have been smaller than present (see scenario in Fig. 7 where tides are reduced to one-third of present), which is incompatible with existing foraminiferal, geomorphic and paleoenvironmental evidence (e.g., Zaremba et al., 2016). Alternatively, if the Roanoke Marshes represented only a partial barrier, then opening of the Outer Banks would cause simultaneous tidal-range change at both Cedar Island and Roanoke Island. For example, Stick (1958) reported that a navigable channel existed through the Roanoke Marshes from early colonial times and was still in use during the Civil War. Importantly, tidal amplification would cause the increase in tidal range to be larger at Roanoke Island (e.g., similar to 5x present) than at Cedar Island (e.g., similar to 2x present; Clunies, 2014). This pattern of tidal-range change would serve to exaggerate rather than resolve differences in RSL between Cedar Island and Roanoke Island (Fig. 7F). Therefore we conclude that tidal-range change in Pamlico Sound caused by opening of the Outer Banks is unlikely to resolve the spatial difference in rates of RSL rise at ~600–1400 CE irrespective of how closed or open the Roanoke Marshes were.

If paleotides at Roanoke Island were larger than present at ~600–1400 CE (but unchanged at Cedar Island), the corrected RSL reconstruction would be lower and improve agreement with the rate of RSL rise at Cedar Island. Moran et al. (2015) used geophysical surveys and recognition of dated litho- and bio-facies to reconstruct paleogeographic changes in Currituck Sound. The presence of calcareous, benthic foraminifera with ecological preferences for high-salinity, estuarine environments showed that Currituck Sound was connected to the Atlantic Ocean from 230 to 600 CE until ~1410 CE by several inlets that subsequently closed (Moran et al., 2015; Robinson and McBride, 2006). With the barrier open, hydrodynamic modeling indicates that tidal range could have reached 1.0 m in southern Currituck Sound, but that tidal range at Roanoke Island was largely unchanged (Moran et al., 2015). This suggests that opening of the Currituck Sound barrier cannot explain the reconstructed RSL difference between Cedar Island and Roanoke Island. Furthermore, the increased abundance of *J. macrescens* at 750–1450 CE (0.96–1.90 m) in the Sand Point core likely indicates decreased salinity around Roanoke Island and a closed barrier configuration based on the distribution of modern foraminifera in the study region (Kemp et al., 2009b; Robinson and McBride, 2006). However, outside of the study region *J. macrescens* does not have a simple relationship to salinity as evidenced by its dominance in normal-salinity, high salt-marsh environments elsewhere (e.g., Edwards and Wright, 2015; Wright et al., 2011). This spatial variability likely reflects the ability of *J. macrescens* to thrive in marginal

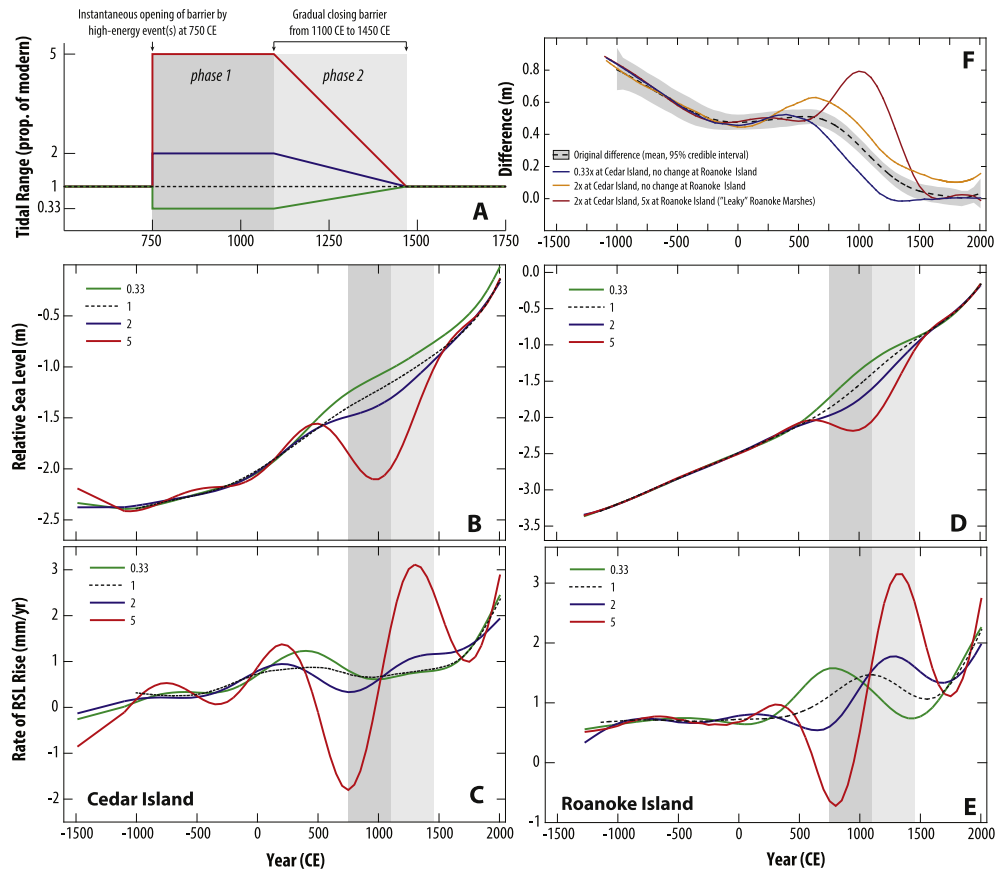


**Fig. 7.** Effect of tidal-range change on the Cedar Island and Roanoke Island relative sea-level (RSL) reconstructions. (A) Simplistic paleotidal scenarios in which tidal range is two (blue line) and five (red line) times larger than present (dashed black line) as a consequence of the Outer Banks barrier being more open. In these scenarios the barrier is instantaneously opened at 750 CE and held open until 1100 CE, after which it returns gradually to a closed configuration and tidal range decreases in a linear fashion through time. These scenarios are intended to be illustrative rather than accurate characterizations of late Holocene changes in coastal geomorphology and paleotidal-range change. For comparison, a third scenario (green line) shows the effect of tidal range that was one-third the size of present. (B, D) Relative sea level and (C, E) rates of relative sea-level rise at Cedar Island and Roanoke Island under the three paleotidal scenarios and under an assumption of no tidal-range change. For clarity of display the curves are the mean estimate from the Errors-In-Variables Integrated Gaussian Process (EIV-IGP) model. (F) Difference in relative sea level between Cedar Island and Roanoke Island under select paleotidal scenarios. The original difference is from the reconstructions that assumed constant tidal regime at both sites. If the Roanoke Marshes represent a barrier, then tidal-range increase occurs at Cedar Island but not Roanoke Island (orange curve) in response to opening of the Outer Banks at ~750 CE. If the Roanoke Marshes are leaky and allow some exchange of water between Albemarle and Pamlico Sounds then tidal-range change is larger at Roanoke Island than it is at Cedar Island (red curve). The blue curve represents an unlikely scenario where tidal range at Cedar Island decreased by two thirds.

environments where other species do not, rather than a predictable relationship to salinity. We conclude that larger-than-present tidal range at Roanoke Island is unlikely to account for the reconstructed RSL difference between Cedar Island and Roanoke Island.

##### 5.5. Dynamic sea-level change in North Carolina and along the U.S. Atlantic coast

Dynamic sea-level changes redistribute existing ocean mass on time scales from days to centuries, resulting in local-to regional-scale RSL trends, but near-zero global mean sea-level change (e.g., Levermann et al., 2005). These trends can arise from changes in ocean currents and/or atmospheric conditions (e.g., Miller and Douglas, 2007). In the North Atlantic Ocean, gyre circulation sustains a sea-level gradient between an elevated sea-surface height toward the center of the North Atlantic gyre and a lower sea-surface height along the coast of North America (e.g., Ezer et al., 2013; Zlotnicki, 1991). This sea-level gradient is proportional to the strength of the Gulf Stream, where weaker/enhanced flow relaxes/enhances the gradient and causes dynamic sea-level rise/fall along the North American coast at locations north of Cape Hatteras (Fig. 1), while locations to the south experience little or no change

(e.g., Bingham and Hughes, 2009; Ezer, 2016; Ezer et al., 2013; McCarthy et al., 2015; Yin and Goddard, 2013). A varied body of paleoceanographic evidence indicates that centennial-scale changes in ocean circulation may have occurred in the North Atlantic Ocean during the late Holocene (e.g., Bianchi and McCave, 1999; Bond et al., 2001; Keigwin, 1996; Kinnard et al., 2011; Lund et al., 2006; Rahmstorf et al., 2015). These changes were likely accompanied by corresponding dynamic sea-level changes.

Atmospheric conditions cause dynamic sea-level change along the Atlantic coast of North America through the inverse barometer effect (e.g., Piecuch and Ponte, 2015) and modified prevailing wind patterns (e.g., Andres et al., 2013; Ezer, 2016; Woodworth et al., 2014). According to Piecuch and Ponte (2015), 10–30% of multi-decadal sea-level trends along the mid-Atlantic and New England coasts since ~1950 CE can be attributed to the inverse barometer effect. Similarly, Piecuch et al. (2016) showed that up to 50% of annual sea-level variability over the period 1980–2010 CE at locations north of Cape Hatteras could be attributed to coastal wind stress. Although these studies focus on instrumental timescales, it is reasonable to assume that longer-lived changes in meteorological conditions accompanied climate phases such as the Medieval Climate Anomaly and Little Ice Age (Mann et al., 2008). For

example, Trouet et al. (2009) reconstructed centennial-scale trends in the North Atlantic Oscillation (NAO) and a long-lived positive phase at ~1000 to 1450 CE likely caused enhanced westerly winds in the North Atlantic (Trouet et al., 2012). However, other proxy-based NAO reconstructions conclude that persistent positive phases characterized ~1200–1400 CE rather than the Medieval Climate Anomaly (Ortega et al., 2015) and evidence for paleo-NAO strength is frequently contradictory. These changing patterns of atmospheric circulation and pressure may have directly forced regional-scale RSL changes and/or induced trends indirectly through interaction with ocean circulation. A RSL reconstruction from Iceland (Saher et al., 2015) indicated that some positive phases of paleo- (Trouet et al., 2009) and historic NAO could be correlated with faster intervals of sea-level rise (~1650 CE, 1850 CE and 1990 CE), but that others (e.g., ~1900 CE) could not be, despite NAO changes of a similar (or larger) magnitude and duration. This result implies a complex relationship between atmospheric forcing and regional RSL change that is likely modulated through the ocean and cryosphere. For example, positive NAO can enhance Atlantic Meridional Overturning Circulation (AMOC; e.g., Delworth and Greatbatch, 2000; Trouet et al., 2012). Therefore NAO phasing may not translate into a recurring pattern of regional-scale RSL change. In North Carolina estuaries, wind-driven water level changes are significantly higher than tides. Therefore dynamic sea-level changes arising from atmospheric changes may be particularly significant in our study region.

Spatial variability of RSL reconstructions from the North American Atlantic coast support the interpretation that dynamic processes in the coupled ocean-atmosphere system caused centennial-scale, non-linear sea-level trends during the late Holocene (Kemp et al., 2015; Kopp et al., 2016). The revised RSL reconstructions from Cedar Island and Roanoke Island further support this inference. Reconstructions from northeastern Florida (Kemp et al., 2014) and Cedar Island (this study) show no evidence for significant, centennial-scale changes in the rate of RSL rise at locations south of Cape Hatteras until the onset of historic rates of rise in the late 19th century (Fig. 8). In contrast, records from locations north of Cape Hatteras in Connecticut (Kemp et al., 2015), southern New Jersey (Kemp et al., 2013a; Cahill et al., 2016), and Roanoke Island (this study) each include a period of faster RSL rise that persists for several centuries during the late Holocene (Fig. 8). First-order RSL differences among sites north and south of Cape Hatteras resemble the spatial pattern predicted to arise from changes in the strength of AMOC (Levermann et al., 2005, Fig. 8). An important caveat to this interpretation is that the models predicting spatial patterns of dynamic sea-level rise commonly have a resolution (grid size) that is too coarse to identify meaningful differences between our two study areas in North Carolina that are separated by ~120 km. Furthermore, Cape Hatteras represents a convenient geographic location for approximating the boundary of dynamic sea-level change rather than a fixed and absolute break point for physical processes.

The North Atlantic Ocean is sensitive to ocean density changes because it is one of the three principal zones where surface waters attain sufficient density to downwell (Kuhlbrodt et al., 2007). Changes to the density of North Atlantic surface water (and subsequently deep-water formation) caused by temperature and/or salinity trends can be accompanied by a change in AMOC strength (Rahmstorf et al., 2015), although Lozier (2012) cautioned against directly equating the rate of deep-water formation with AMOC strength. Weaker/stronger AMOC would induce dynamic sea-level rise/fall north of Cape Hatteras (Levermann et al., 2005). Therefore, increased rates of RSL at Roanoke Island at ~600–1100 CE could reflect AMOC weakening, while the decreasing rates of RSL rise at ~1100–1500 CE would indicate (re)strengthening AMOC. However,

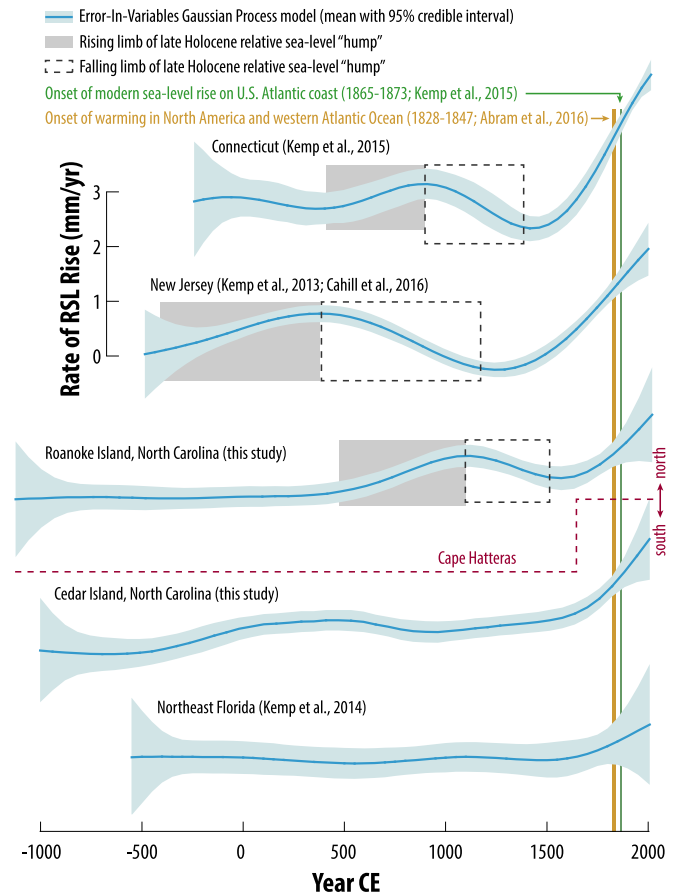


**Fig. 8.** Rates of relative sea-level (RSL) rise reconstructed from a suite of sites (arranged by latitude) along the U.S. Atlantic coast. All records are presented at a consistent scale, but offset from one another to aid comparison, no correction was made for spatially-variable glacio-isostatic adjustment. At sites north of Cape Hatteras there is a characteristic rising (grey shaded interval) and falling (interval shown by dashed lines) limb during the late Holocene. This feature is absent at locations south of Cape Hatteras suggesting that ocean/atmosphere dynamics were an important driver of reconstructed trends. All reconstructions show that the modern rate of rise was initiated shortly after anthropogenic warming commenced and is the fastest rate of rise recorded during the late Holocene.

there are three outstanding limitations of this interpretation.

Firstly, the reported sensitivity of Atlantic coast sea level to reduced AMOC strength (1–5 cm/Sv; e.g., Bingham and Hughes, 2009; Ezer, 2001; Goddard et al., 2015; Levermann et al., 2005; Lorbacher et al., 2010) is too low to adequately explain reconstructed RSL changes. Given their proximity to one another, the relative sensitivity of RSL at Cedar Island and Roanoke Island to AMOC strength is likely low. To attribute the difference in RSL between Cedar Island and Roanoke Island (~15 cm after accounting for GIA; Fig. 5D) solely to weaker AMOC would require a reduction in strength by up to 15 Sv, compared to a modern strength of ~32 Sv in the Florida Strait (e.g., Bryden et al., 2005). As far as we are aware there is no paleoceanographic evidence to support multi-centennial weakening of AMOC by this magnitude in the late Holocene. Furthermore, the RSL induced by such a change in AMOC strength would likely be larger still at sites further north than Roanoke Island, which is not supported by existing reconstructions (Fig. 8). However, if simultaneous contributions from atmospheric processes occurred (e.g., Piecuch and Ponte, 2015) then this apparent discrepancy may be partially resolved. In addition, if AMOC variability is caused by, or causes, change in ocean mass through melting or growth of land-based ice, then the resulting

pattern of sea-level change will include the spatial fingerprint of ice volume changes. For example, melting of the Greenland Ice Sheet causes larger RSL change at distal sites (e.g., Florida) than at proximal sites (e.g., Canadian Maritimes; Mitrovica et al., 2011), which would counteract the spatial expression of ocean dynamic RSL rise that is greater north of Cape Hatteras than it is to the south. Therefore, if ocean dynamic RSL changes were initiated, or accompanied, by changes in land-based ice volume in the northern hemisphere, then the spatial expression of both processes may serve to mask or distort one another. This relationship between RSL change caused by AMOC and melting of land-based ice serves to make all latitudes on the Atlantic coast more sensitive to RSL rise. Secondly, other proxies show little or contradictory evidence for significant changes in AMOC strength during this interval. For example, Bond et al. (2001) reconstructed decreasing drift ice in the North Atlantic Ocean at ~750–1050 CE (although age uncertainties were large) and proposed that it was accompanied by increased production of North Atlantic Deep Water (potentially stronger AMOC and reduced RSL rise). This was followed (~1050–1350 CE) by increasing drift ice that potentially reflects weaker AMOC and increased RSL rise. In contrast, Trouet et al. (2012) proposed that a positive NAO phase at ~1000 CE to ~1450 CE contributed to stronger AMOC, while the AMOC reconstruction of Rahmstorf et al. (2015) does not show significant trends over the period ~800–1400 CE. Thirdly, and perhaps most significantly, the timing and magnitude of the RSL rise and subsequent fall varies among records, which is inconsistent with a common and/or simultaneous driving mechanism. In Connecticut, the rate of RSL rise exceeded the contribution from GIA between ~500 CE and 1100 CE (peak at ~800 CE), compared to 0–1000 CE (peak at ~600 CE) in New Jersey and 600–1400 CE (peak at ~1100 CE) at Roanoke Island (Fig. 8). Model predictions of AMOC-induced sea-level change suggest that the RSL rise should be larger at sites such as Connecticut than at Roanoke Island, yet the reconstructions do not show this pattern. Furthermore, the size of the RSL difference between Cedar Island and Roanoke Island, given their proximity to one another and to Cape Hatteras, causes us to question the significance of AMOC as a driver of late Holocene sea-level change.

In the specific case of North Carolina, prevailing winds sustain significant sea-level gradients within Pamlico and Albemarle Sounds, in part as a consequence of large fetch and small astronomical tides (e.g., Reed et al., 2008). The modern distribution of salt-marsh foraminifera reflects this phenomenon, with *in situ* assemblages occurring at elevations considerably above highest astronomical tide (Kemp et al., 2009b), while datasets from elsewhere indicate that the highest occurrence of foraminifera and highest astronomical tides occur at similar elevations (Wright et al., 2011). As such our modern training set of foraminifera that is used to delimit high salt-marsh environments reflects a flooding regime comprised of tidal and wind-driven components. As with our starting assumption about stationary tidal range, the RSL reconstructions that we produced inherently assumed that inundation frequency and duration caused by wind-driven water levels remained constant through time. However, changing prevailing winds (strength and/or direction) could induce substantial and potentially local-scale (e.g., through site aspect) RSL changes in North Carolina. Indeed, hydrodynamic modeling indicates that winds continue to exert a significant influence on local water levels even after extensive segmentation of the Outer Banks barrier islands. Since the Albemarle basin (and its corresponding fetch) is larger than the Pamlico basin, the effect of wind-driven water levels is potentially larger at Roanoke Island than it is at Cedar Island, which may help to explain the reconstructed RSL difference. Additional work is needed to more reliably isolate regional and local-scale signals from RSL records along the Atlantic coast of

North America to better estimate contributions from driving mechanisms that are linked to one another through a complex network of feedback mechanisms. This work should include efforts to increase confidence in how well RSL reconstructions represent regional-scale trends through replication within and among study sites. In North Carolina, distinguishing dynamic sea-level changes caused by oceanographic processes from those caused by atmospheric processes will be an important step in understanding the history of RSL change in the North Atlantic Ocean.

## 6. Conclusions

Near-continuous and precise late Holocene (past ~3000 years) relative sea-level (RSL) reconstructions derived from salt-marsh sediment on the Atlantic coast of North America provide an opportunity to determine the driving mechanisms of regional-scale sea-level trends on decadal to millennial timescales. In support of this goal, we extended the record of RSL change in North Carolina by reinterpreting existing data and by collecting and analyzing two new sediment cores with the aim of better understanding RSL trends within North Carolina and along the U.S. Atlantic coast with particular emphasis on the period prior to ~1100 CE. We used foraminifera as sea-level indicators by applying a binary classification to assemblages preserved in each core. High salt-marsh assemblages were assumed to form between mean high water and the highest occurrence of foraminifera in the study region. No low salt-marsh assemblages were identified in the cores that we analyzed. The age-depth history of the new cores was established through radiocarbon dating of plant macrofossils. At Cedar Island, RSL rose by ~2.4 m during the past ~3000 years, compared to ~3.3 m at Roanoke Island. The difference between the two reconstructions decreased through time in a non-linear fashion that cannot be adequately explained by spatially-variable GIA, which caused RSL rise to be 0.1–0.2 mm/yr faster at Roanoke Island than at Cedar Island. An important feature of the extended North Carolina RSL reconstructions is a period (~600–1100 CE) of accelerating RSL rise at Roanoke Island that is absent at Cedar Island. Paleogeographic and microfaunal evidence coupled with existing hydrodynamic and geotechnical models indicate that this spatial variability cannot be explained by sediment compaction, sediment dynamics, or tidal-range change. The pattern of sea-level variability reconstructed within North Carolina and at other sites from Florida to Connecticut suggests that dynamic oceanic and/or atmospheric circulation contributed to late Holocene RSL change in the North Atlantic Ocean on local and regional spatial scales.

## Acknowledgments

We thank Stefan Rahmstorf, Matthew Brain, Hannah Thornberg, Ray Tichenor, and Nina Shmorhun for their help in the field and Jerry Mitrovica for providing GIA predictions. Woodson first examined the sedimentary successions beneath the Hill Point site as part of her undergraduate thesis at Bryn Mawr College under the guidance of Barber. Kegel analyzed the Hill Point core for her Masters thesis at East Carolina University under the guidance of Culver, Leorri and Kemp. This work was supported by NSF award OCE-1458921 to Kemp, EAR-1402017, EAR-1322742 to Culver, OCE-1130843 to Mallinson and OCE-1458904 to BPH. Bernhardt is funded through the USGS Climate and Land Use R&D program. Any use of trade, firm, or product names is for descriptive purposes only and does not imply endorsement by the U.S. Government. Thorough and constructive comments from two reviewers helped to improve this study and manuscript. It is a contribution to PALSEA 2 and IGCP Project 639, “Sea-level change from minutes to millennia”.

## Appendix A. Supplementary data

Supplementary data related to this article can be found at <http://dx.doi.org/10.1016/j.quascirev.2017.01.012>.

### Appendix. Tabulated data from the Tump Point, Hill Point, Sand Point Russian and SPVC-2 cores. The dictionary tab provides a definition for all abbreviations.

Depth	Lower depth (cm) in core of 1-cm thick sample
JM	<i>Jadammina macrescens</i> %
HW	<i>Haplophragmoides wilberti</i> %
TI	<i>Trochammina inflata</i> %
TC	<i>Tiphrotracha comprimata</i> %
HM	<i>Haplophragmoides manilaensis</i> %
AM	<i>Arenoparella mexicana</i> %
PL	<i>Pseudothurammina limentis</i> %
MP	<i>Miliammina petita</i> %
MF	<i>Miliammina fusca</i> %
SL	<i>Siphotrochammina lobata</i> %
RN	<i>Reophax nana</i> %
AI	<i>Ammonoastuta inepta</i> %
As	<i>Ammotium salsum</i> %
AP	<i>Ammobaculites</i> spp. %
AB	<i>Trochammina salsa</i> %
Ts	<i>Trochammina irregularis</i> %
TR	<i>Trochammina rotaliformis</i> %
MO	<i>Miliammina obliqua</i> %
HB	<i>Haplophragmoides bonplandi</i> %
Elevation (m MTL)	Sample elevation with respect to modern and local mean tide level (meters)
PME (m MTL)	Paleomarrow elevation expressed with respect to mean tide level (meters)
PME Error (m)	Paleomarrow elevation uncertainty expressed in meters (assumed to be $\sim 2\sigma$ )
RSL (m)	Relative sea level (meters); Elevation less paleomarrow elevation
RSL Error (m)	Relative sea level uncertainty (meters, assumed to be $\sim 2\sigma$ )
AD2.5	2.5% interval for Bchron age-depth model (year AD)
AD10	10% interval for Bchron age-depth model (year AD)
AD50	50% interval for Bchron age-depth model (year AD)
AD90	90% interval for Bchron age-depth model (year AD)
AD97.5	97.5% interval for Bchron age-depth model (year AD)

## References

- Adams, D.A., 1963. Factors influencing vascular plant zonation in North Carolina salt marshes. *Ecology* 44, 445.
- Andres, M., Gawarkiewicz, G.G., Toole, J.M., 2013. Interannual sea level variability in the western North Atlantic: regional forcing and remote response. *Geophys. Res. Lett.* 40, 5915–5919.
- Anisfeld, S.C., Tobin, M.J., Benoit, G., 1999. Sedimentation rates in flow-restricted and restored salt marshes in Long Island sound. *Estuaries* 22, 231–244.
- Appleby, P.G., Oldfield, F., 1992. Application of Lead-210 to sedimentation studies. In: Ivanovich, M., Harmon, R.S. (Eds.), *Uranium Series Disequilibrium: Applications to Environmental Problems*. Clarendon Press, pp. 731–778.
- Argus, D.F., Peltier, W.R., Drummond, R., Moore, A.W., 2014. The Antarctic component of postglacial rebound model ICE-6G\_C (VM5a) based upon GPS positioning, exposure age dating of ice thicknesses and relative sea level histories. *Geophys. J. Int.* 198, 537–563.
- Barlow, N.L.M., Shennan, I., Long, A.J., Gehrels, W.R., Saher, M.H., Woodroffe, S.A., Hillier, C., 2013. Salt marshes as late Holocene tide gauges. *Glob. Planet. Change* 106, 90–110.
- Bianchi, G.G., McCave, I.N., 1999. Holocene periodicity in North Atlantic climate and deep-ocean flow south of Iceland. *Nature* 397, 515–517.
- Bingham, R.J., Hughes, C.W., 2009. Signature of the Atlantic meridional overturning circulation in sea level along the east coast of North America. *Geophys. Res. Lett.* 36, L02603.
- Bloom, A.L., 1964. Peat accumulation and compaction in Connecticut coastal marsh. *J. Sediment. Res.* 34, 599–603.
- Bond, G., Kromer, B., Beer, J., Muscheler, R., Evans, M.N., Showers, W., Hoffmann, S., Lotti-Bond, R., Hajdas, I., Bonani, G., 2001. Persistent solar influence on North Atlantic climate during the Holocene. *Science* 294, 2130–2136.
- Brain, M.J., Long, A.J., Woodroffe, S.A., Petley, D.N., Milledge, D.G., Parnell, A.C., 2012. Modelling the effects of sediment compaction on salt marsh reconstructions of recent sea-level rise. *Earth Planet. Sci. Lett.* 345–348, 180–193.
- Brain, M., Kemp, A.C., Horton, B.P., Culver, S.J., Parnell, A.C., Cahill, N., 2015. Quantifying the contribution of sediment compaction to late Holocene salt-marsh sea-level reconstructions, North Carolina, USA. *Quat. Res.* 83, 41–51.
- Brinson, M.M., 1991. Ecology of a nontidal brackish marsh in coastal North Carolina. In: Brinson, M.M. (Ed.), *National Wetlands Research Center Open File Report 91-03*, p. 398. U.S. Fish and Wildlife Service.
- Brugam, R.B., 1978. Pollen indicators of land-use change in southern Connecticut. *Quat. Res.* 9, 349–362.
- Bryden, H.L., Longworth, H.R., Cunningham, S.A., 2005. Slowing of the Atlantic meridional overturning circulation at 25 N. *Nature* 438, 655–657.
- Cahill, N., Kemp, A.C., Horton, B.P., Parnell, A.C., 2015. Modeling sea-level change using errors-in-variables integrated Gaussian processes. *Ann. Appl. Stat.* 9, 547–571.
- Cahill, N., Kemp, A.C., Horton, B.P., Parnell, A.C., 2016. A Bayesian hierarchical model for reconstructing relative sea level: from raw data to rates of change. *Climate of the Past* 12 (2), 525–542.
- Clunies, G.J., 2014. Hydrodynamics of a Large and Shallow Back-barrier Estuarine System and Responses to Long-term Changes in Geomorphology. Department of Civil Engineering, Queens University, p. 99.
- Cooper, S., McGlothlin, S., Madritch, M., Jones, D., 2004. Paleocological evidence of human impacts on the Neuse and Pamlico estuaries of North Carolina, USA. *Estuaries Coasts* 27, 617–633.
- Craft, C., Broome, S., Campbell, C., 2002. Fifteen years of vegetation and soil development after brackish-water marsh creation. *Restor. Ecol.* 10, 248–258.
- Culver, S.J., Horton, B.P., 2005. Infaunal marsh foraminifera from the outer Banks, North Carolina, USA. *J. Foraminif. Res.* 35, 148–170.
- Culver, S., Grand-Pre, C., Mallinson, D., Riggs, S., Corbett, D.R., Foley, J., Hale, M., Metger, L., Ricardo, J., Rosenberger, J., Smith, C.G., Smith, C.W., Snyder, S.W., Twamley, D., Farrell, K., Horton, B., 2007. Late Holocene barrier island collapse; outer Banks, North Carolina, USA. *Sediment. Rec.* 5, 4–8.
- Davis, J.L., Mitrovica, J.X., 1996. Glacial isostatic adjustment and the anomalous tide gauge record of eastern North America. *Nature* 379, 331–333.
- De Vleeschouwer, D., Parnell, A.C., 2014. Reducing time-scale uncertainty for the Devonian by integrating astrochronology and Bayesian statistics. *Geology* 42, 491–494.
- Delaune, R.D., Patrick, W.H., Buresh, R.J., 1978. Sedimentation rates determined by <sup>137</sup>Cs dating in a rapidly accreting salt marsh. *Nature* 275, 532–533.
- Delworth, T.L., Greatbatch, R.J., 2000. Multidecadal thermohaline circulation variability driven by atmospheric surface flux forcing. *J. Clim.* 13, 1481–1495.
- Edwards, R.J., Wright, A.J., 2015. Foraminifera. In: Shennan, I., Long, A.J., Horton, B.P. (Eds.), *Handbook of Sea-level Research*. John Wiley & Sons, Chichester, pp. 191–217.
- Eleuterius, L., 1976a. The distribution of *Juncus roemerianus* in the salt marshes of North America. *Chesap. Sci.* 17, 289–292.
- Eleuterius, L., 1976b. Vegetative morphology and anatomy of the salt-marsh rush *Juncus roemerianus*. *Gulf Res. Rep.* 5, 1–10.
- Eleuterius, L., 2000. *Tidal Marsh Plants*. Pelican Publishing, Gretna, Louisiana.
- Engelhart, S.E., Horton, B.P., Douglas, B.C., Peltier, W.R., Tornqvist, T.E., 2009. Spatial variability of late Holocene and 20th century sea-level rise along the Atlantic coast of the United States. *Geology* 37, 1115–1118.
- Ezer, T., 2001. Can long-term variability in the Gulf Stream Transport be inferred from sea level? *Geophys. Res. Lett.* 28, 1031–1034.
- Ezer, T., 2016. Can the Gulf Stream induce coherent short-term fluctuations in sea level along the US East Coast? A modeling study. *Ocean. Dyn.* 66, 207–220.
- Ezer, T., Atkinson, L.P., Corlett, W.B., Blanco, J.L., 2013. Gulf Stream's induced sea level rise and variability along the U.S. mid-Atlantic coast. *J. Geophys. Res. Oceans* 118, 685–697.
- Fatela, F., Taborda, R., 2002. Confidence limits of species proportions in microfossil assemblages. *Mar. Micropaleontol.* 45, 169–174.
- Goddard, P.B., Yin, J., Griffies, S.M., Zhang, S., 2015. An extreme event of sea-level rise along the Northeast coast of North America in 2009–2010. *Nat. Commun.* 6, 6346.
- Grand Pre, C., Culver, S.J., Mallinson, D.J., Farrell, K.M., Corbett, D.R., Horton, B.P., Hillier, C., Riggs, S.R., Snyder, S.W., Buzas, M.A., 2011. Rapid Holocene coastal change revealed by high-resolution micropaleontological analysis, Pamlico Sound, North Carolina, USA. *Quat. Res.* 76, 319–334.
- Grimm, E.C., 1987. CONISS: a FORTRAN 77 program for stratigraphically constrained cluster analysis by the method of incremental sum of squares. *Comput. Geosci.* 13, 13–35.
- Haslett, J., Parnell, A., 2008. A simple monotone process with application to radiocarbon-dated depth chronologies. *J. R. Stat. Soc. Ser. C Appl. Stat.* 57, 399–418.
- Hawkes, A.D., Horton, B.P., Nelson, A.R., Hill, D.F., 2010. The application of intertidal foraminifera to reconstruct coastal subsidence during the giant Cascadia earthquake of AD 1700 in Oregon, USA. *Quat. Int.* 221, 116–140.
- Hess, K.W., Spargo, E.A., Wong, A., White, S.A., Gill, S.K., 2005. VDatum for Central Coastal North Carolina Tidal Datums, Marine Grids, and Sea Surface Topography. National Oceanic and Atmospheric Administration, p. 46.

- Hill, D.F., Griffiths, S.D., Peltier, W.R., Horton, B.P., Tornqvist, T.E., 2011. High-resolution numerical modeling of tides in the western Atlantic, Gulf of Mexico, and Caribbean sea during the Holocene. *J. Geophys. Res.* 116, C10014.
- Hobbs, N., 1986. Mire morphology and the properties and behaviour of some British and foreign peats. *Q. J. Eng. Geol. Hydrogeol.* 19, 7–80.
- Horton, B.P., Culver, S.J., 2008. Modern intertidal foraminifera of the Outer Banks, North Carolina, U.S.A., and their applicability for sea-level studies. *J. Coast. Res.* 24, 1110–1125.
- Horton, B.P., Edwards, R.J., 2006. Quantifying Holocene Sea-level Change Using Intertidal Foraminifera: Lessons from the British Isles. Cushman Foundation for Foraminiferal Research, Washington D.C.
- Jackson, S.T., Williams, J.W., 2004. Modern analogs in Quaternary paleoecology: here today, gone yesterday, gone tomorrow? *Annu. Rev. Earth Planet. Sci.* 32, 495–537.
- Juggins, S., Birks, H.J.B., 2012. Quantitative environmental reconstructions from biological data. In: Birks, H.J.B., Lotter, A.F., Juggins, S., Smol, J.P. (Eds.), *Tracking Environmental Change Using Lake Sediments: Data Handling and Numerical Techniques*. Springer, Dordrecht, pp. 431–494.
- Kaye, C.A., Barghoorn, E.S., 1964. Late Quaternary sea-level change and crustal rise at Boston, Massachusetts, with notes on the autocompaction of peat. *Geol. Soc. Am. Bull.* 75, 63–80.
- Kegel, J., 2015. Extension of the Late Holocene Sea-level Record in North Carolina, USA. Department of Geological Sciences. East Carolina University, p. 70. Unpublished MSc Thesis.
- Keigwin, L.D., 1996. The little ice age and medieval warm period in the Sargasso sea. *Science* 274, 1503–1508.
- Kemp, A.C., Horton, B.P., Corbett, D.R., Culver, S.J., Edwards, R.J., van de Plassche, O., 2009a. The relative utility of foraminifera and diatoms for reconstructing late Holocene sea-level change in North Carolina, USA. *Quat. Res.* 71, 9–21.
- Kemp, A.C., Horton, B.P., Culver, S.J., 2009b. Distribution of modern salt-marsh foraminifera in the Albemarle-Pamlico estuarine system of North Carolina, USA: implications for sea-level research. *Mar. Micropaleontol.* 72, 222–238.
- Kemp, A.C., Horton, B.P., Culver, S.J., Corbett, D.R., van de Plassche, O., Gehrels, W.R., Douglas, B.C., Parnell, A.C., 2009c. Timing and magnitude of recent accelerated sea-level rise (North Carolina, United States). *Geology* 37, 1035–1038.
- Kemp, A.C., Vane, C.H., Horton, B.P., Culver, S.J., 2010. Stable carbon isotopes as potential sea-level indicators in salt marshes, North Carolina, USA. *Holocene* 20, 623–636.
- Kemp, A.C., Horton, B., Donnelly, J.P., Mann, M.E., Vermeer, M., Rahmstorf, S., 2011. Climate related sea-level variations over the past two millennia. *Proc. Natl. Acad. Sci.* 108, 11017–11022.
- Kemp, A.C., Vane, C.H., Horton, B.P., Engelhart, S.E., Nikitina, D., 2012. Application of stable carbon isotopes for reconstructing salt-marsh floral zones and relative sea level, New Jersey, USA. *J. Quat. Sci.* 27, 404–414.
- Kemp, A.C., Horton, B.P., Vane, C.H., Corbett, D.R., Bernhardt, C.E., Engelhart, S.E., Anisfeld, S.C., Parnell, A.C., Cahill, N., 2013a. Sea-level change during the last 2500 years in New Jersey, USA. *Quat. Sci. Rev.* 81, 90–104.
- Kemp, A.C., Nelson, A.R., Horton, B.P., 2013b. Radiocarbon dating of plant macrofossils in tidal marsh sediment. In: Schroder, J. (Ed.), *Treatise on Geomorphology*. Academic Press, San Diego, CA, pp. 370–388.
- Kemp, A.C., Bernhardt, C.E., Horton, B.P., Vane, C.H., Peltier, W.R., Hawkes, A.D., Donnelly, J.P., Parnell, A.C., Cahill, N., 2014. Late Holocene sea- and land-level change on the U.S. southeastern Atlantic coast. *Mar. Geol.* 357, 90–100.
- Kemp, A.C., Hawkes, A.D., Donnelly, J.P., Vane, C.H., Horton, B.P., Hill, T.D., Anisfeld, S.C., Parnell, A.C., Cahill, N., 2015. Relative sea-level change in Connecticut (USA) during the last 2200 years. *Earth Planet. Sci. Lett.* 428, 217–229.
- Kinnard, C., Zdanowicz, C.M., Fisher, D.A., Isaksson, E., de Vernal, A., Thompson, L.G., 2011. Reconstructed changes in Arctic sea ice over the past 1,450 years. *Nature* 479, 509–512.
- Kirwan, M.L., Murray, A.B., 2008. Tidal marshes as the disequilibrium landscapes: lags between morphology and Holocene sea level change. *Geophys. Res. Lett.* 35, L24401.
- Kopp, R.E., 2013. Does the mid-Atlantic United States sea level acceleration hot spot reflect ocean dynamic variability? *Geophys. Res. Lett.* 40, 3981–3985.
- Kopp, R.E., Kemp, A.C., Bitterman, K., Horton, B.P., Donnelly, J.P., Gehrels, W.R., Hay, C., Mitrovica, J.X., Morrow, E., Rahmstorf, S., 2016. Temperature-driven global sea-level variability in the Common Era. *Proc. Natl. Acad. Sci.* 113, E1434–E1441.
- Kuhlbrodt, T., Griesel, A., Montoya, M., Levermann, A., Hofmann, M., Rahmstorf, S., 2007. On the driving processes of the Atlantic meridional overturning circulation. *Rev. Geophys.* 45, RG2001.
- Levermann, A., Griesel, A., Hofmann, M., Montoya, M., Rahmstorf, S., 2005. Dynamic sea level changes following changes in the thermohaline circulation. *Clim. Dyn.* 24, 347–354.
- Long, A.J., Barlow, N.L.M., Gehrels, W.R., Saher, M.H., Woodworth, P.L., Scaife, R.G., Brain, M.J., Cahill, N., 2014. Contrasting records of sea-level change in the eastern and western North Atlantic during the last 300 years. *Earth Planet. Sci. Lett.* 388, 110–122.
- Lorbacher, K., Dengg, J., Böning, C.W., Biastoch, A., 2010. Regional patterns of sea level change related to interannual variability and multidecadal trends in the Atlantic Meridional Overturning Circulation. *J. Clim.* 23, 4243–4254.
- Lozier, M.S., 2012. Overturning in the north Atlantic. *Annu. Rev. Mar. Sci.* 4, 291–315.
- Lund, D.C., Lynch-Stieglitz, J., Curry, W.B., 2006. Gulf Stream density structure and transport during the last millennium. *Nature* 444, 601–604.
- Mallinson, D.J., Culver, S.J., Riggs, S.R., Walsh, J.P., Ames, D., Smith, C.W., 2008. Past, Present and Future Inlets of the Outer Banks Barrier Islands, North Carolina. East Carolina University, p. 22.
- Mallinson, D.J., Smith, C.W., Culver, S.J., Riggs, S.R., Ames, D., 2010. Geological characteristics and spatial distribution of paleo-inlet channels beneath the Outer Banks barrier islands, North Carolina, USA. *Estuarine, Coast. Shelf Sci.* 88, 175–189.
- Mallinson, D.J., Smith, C.W., Mahan, S., Culver, S.J., McDowell, K., 2011. Barrier island response to late Holocene climate events, North Carolina, USA. *Quat. Res.* 76, 46–57.
- Mann, M.E., Zhang, Z., Hughes, M.K., Bradley, R.S., Miller, S.K., Rutherford, S., Ni, F., 2008. Proxy-based reconstructions of hemispheric and global surface temperature variations over the past two millennia. *Proc. Natl. Acad. Sci.* 105, 13252–13257.
- McAndrews, J.H., 1988. Human disturbance of North American forests and grasslands: the fossil pollen record. In: Huntley, B., Webb, T. (Eds.), *Vegetation History*. Springer Netherlands, Dordrecht, pp. 673–697.
- McCarthy, G.D., Haigh, I.D., Hirschi, J.J.M., Grist, J.P., Smeed, D.A., 2015. Ocean impact on decadal Atlantic climate variability revealed by sea-level observations. *Nature* 521, 508–510.
- Miller, L., Douglas, B.C., 2007. Gyre-scale atmospheric pressure variations and their relation to 19th and 20th century sea level rise. *Geophys. Res. Lett.* 34, L16602.
- Mitrovica, J.X., Tamisiea, M.E., Davis, J.L., Milne, G.A., 2001. Recent mass balance of polar ice sheets inferred from patterns of global sea-level change. *Nature* 409, 1026–1029.
- Mitrovica, J.X., Gomez, N., Morrow, E., Hay, C., Latychev, K., Tamisiea, M.E., 2011. On the robustness of predictions of sea level fingerprints. *Geophys. J. Int.* 187, 729–742.
- Moran, K.L., Mallinson, D.J., Culver, S.J., Leorri, E., Mulligan, R.P., 2015. Late Holocene evolution of Currituck Sound, North Carolina, USA: environmental change driven by sea-level rise, storms, and barrier island morphology. *J. Coast. Res.* 31, 827–841.
- Morris, J.T., Sundareshwar, P.V., Nietch, C.T., Kjerfve, B., Cahoon, D.R., 2002. Response of coastal wetlands to rising sea level. *Ecology* 83, 2869–2877.
- Niering, W.A., Warren, R.S., Weymouth, C.G., 1977. Our Dynamic Tidal Marshes: Vegetation Changes as Revealed by Peat Analysis, 22 ed, p. 12. The Connecticut Arboretum Bulletin.
- Ortega, P., Lehner, F., Swingedouw, D., Masson-Delmotte, V., Raible, C.C., Casado, M., Yiou, P., 2015. A model-tested North Atlantic Oscillation reconstruction for the past millennium. *Nature* 523, 71–74.
- Overpeck, J.T., Webb, T., Prentice, I.C., 1985. Quantitative interpretation of fossil pollen spectra: dissimilarity coefficients and the method of modern analogs. *Quat. Res.* 23, 87–108.
- O'Connor, M.P., Riggs, S.R., Winston, D., 1972. Recent estuarine sediment history of the Roanoke Island area, North Carolina. *Geol. Soc. Am. Memoirs* 133, 453–464.
- Parnell, A.C., Gehrels, W.R., 2015. Using chronological models in late Holocene sea-level reconstructions from saltmarsh sediments. In: Shennan, I., Long, A.J., Horton, B.P. (Eds.), *Handbook of Sea-level Research*. John Wiley & Sons, pp. 500–513.
- Parnell, A.C., Haslett, J., Allen, J.R.M., Buck, C.E., Huntley, B., 2008. A flexible approach to assessing synchronicity of past events using Bayesian reconstructions of sedimentation history. *Quat. Sci. Rev.* 27, 1872–1885.
- Parnell, A.C., Buck, C.E., Doan, T.K., 2011. A review of statistical chronology models for high-resolution, proxy-based Holocene palaeoenvironmental reconstruction. *Quat. Sci. Rev.* 30, 2948–2960.
- Peltier, W.R., 1996. Global sea level rise and glacial isostatic adjustment: an analysis of data from the east coast of North America. *Geophys. Res. Lett.* 23, G100848.
- Peltier, W.R., 2004. Global glacial isostasy and the surface of the ice-age Earth: the ICE-5G (VM2) model and GRACE. *Annu. Rev. Earth Planet. Sci.* 32, 111–149.
- Pieuch, C.G., Ponte, R.M., 2015. Inverted barometer contributions to recent sea level changes along the northeast coast of North America. *Geophys. Res. Lett.* 42, 5918–5925.
- Pieuch, C.G., Dangendorf, S., Ponte, R.M., Marcos, M., 2016. Annual sea level changes on the North American northeast coast: influence of local winds and barotropic motions. *J. Clim.* 29, 4801–4816.
- Powrie, W., 2013. *Soil Mechanics: Concepts and Applications*. CRC Press, Boca Raton, FL.
- Punmia, B., Jain, A.K., 2005. *Soil Mechanics and Foundations*. Laxmi Publications, New Delhi, India.
- Rahmstorf, S., Box, J.E., Feulner, G., Mann, M.E., Robinson, A., Rutherford, S., Schaffernicht, E.J., 2015. Exceptional twentieth-century slowdown in Atlantic Ocean overturning circulation. *Nat. Clim. Change* 5, 475–480.
- Reed, R.E., Dickey, D.A., Burkholder, J.M., Kinder, C.A., Brownie, C., 2008. Water level variations in the Neuse and Pamlico Estuaries, North Carolina due to local and remote forcing. *Estuarine, Coast. Shelf Sci.* 76, 431–446.
- Reimer, P.J., Brown, T.A., Reimer, R.W., 2004. Discussion: reporting and calibration of post-bomb <sup>14</sup>C data. *Radiocarbon* 46, 1299–1304.
- Reimer, P.J., Bard, E., Bayliss, A., Beck, J.W., Blackwell, P.G., Bronk Ramsey, C., Grootes, P.M., Guilderson, T.P., Hafflidason, H., Hajdas, I., Hatté, C., Heaton, T.J., Hoffmann, D.L., Hogg, A.G., Hughes, K.A., Kaiser, K.F., Kromer, B., Manning, S.W., Niu, M., Reimer, R.W., Richards, D.A., Scott, E.M., Southon, J.R., Staff, R.A., Turney, C.S.M., van der Plicht, J., 2013. IntCal13 and Marine13 radiocarbon age calibration curves 0–50,000 Years cal BP. *Radiocarbon* 55, 1869–1887.
- Riggs, S., 2002. Life at the edge of North Carolina's coastal system: the geologic controls. In: Beal, C.A.P. (Ed.), *Life at the Edge of the Sea: Essays on North*

- Carolina's Coast and Coastal Culture. Coastal Carolina Press, pp. 63–95.
- Riggs, S.R., Ames, D., 2003. Drowning the North Carolina Coast: Sea-level Rise and Estuarine Dynamics, p. 152. Raleigh, NC.
- Riggs, S.R., Rudolph, G.L., Ames, D., 2000. Erosion Scour and Geologic Evolution of the Croatan Sound, Northeastern North Carolina. North Carolina Department of Transportation, Raleigh, NC, p. 115.
- Robinson, M.M., McBride, R.A., 2006. Benthic foraminifera from a relict flood tidal delta along the Virginia/North Carolina Outer Banks. *Micropaleontology* 52, 67–80.
- Roy, K., Peltier, W.R., 2015. Glacial isostatic adjustment, relative sea level history and mantle viscosity: reconciling relative sea level model predictions for the U.S. East coast with geological constraints. *Geophys. J. Int.* 201, 1156–1181.
- Saheer, M.H., Gehrels, W.R., Barlow, N.L.M., Long, A.J., Haigh, I.D., Blaauw, M., 2015. Sea-level changes in Iceland and the influence of the North Atlantic Oscillation during the last half millennium. *Quat. Sci. Rev.* 108, 23–36.
- Scott, D.B., Medioli, F.S., 1978. Vertical zonations of marsh foraminifera as accurate indicators of former sea levels. *Nature* 272, 528–531.
- Sharma, P., Gardner, L., Moore, W., Bollinger, A., 1987. Sedimentation and bioturbation in a salt marsh as revealed by  $^{210}\text{Pb}$ ,  $^{137}\text{Cs}$ , and  $^7\text{Be}$  studies. *Limnol. Oceanogr.* 32, 313–326.
- Stahle, D.W., Cleaveland, M.K., Hehr, J.G., 1988. North Carolina climate changes reconstructed from tree rings: AD 372 to 1985. *Science* 240, 1517–1519.
- Stick, D., 1958. The Outer Banks of North Carolina 1584–1958. University of North Carolina Press, Chapel Hill, NC.
- Stuiver, M., Polach, H.A., 1977. Reporting of  $^{14}\text{C}$  data. *Radiocarbon* 19, 355–363.
- Traverse, A., 2007. *Paleopalynology*. Springer.
- Troels-Smith, J., 1955. Characterisation of unconsolidated sediments. *Danmarks Geol. Unders.* IV, 39–71.
- Trouet, V., Esper, J., Graham, N.E., Baker, A., Scourse, J.D., Frank, D.C., 2009. Persistent positive North Atlantic oscillation mode dominated the medieval climate anomaly. *Science* 324, 78–80.
- Trouet, V., Scourse, J.D., Raible, C.C., 2012. North Atlantic storminess and Atlantic Meridional Overturning Circulation during the last millennium: reconciling contradictory proxy records of NAO variability. *Glob. Planet. Change* 84–85, 48–55.
- Turekian, K.K., Cochran, J.K., Benninger, L.K., Aller, R.C., 1980. The sources and sinks of nuclides in Long Island Sound. In: Saltzman, B. (Ed.), *Estuarine Physics and Chemistry: Studies in Long Island Sound*, pp. 129–164. Academic, New York.
- van de Plassche, O., Wright, A.J., Horton, B.P., Engelhart, S.E., Kemp, A.C., Mallinson, D., Kopp, R.E., 2014. Estimating tectonic uplift of the Cape Fear Arch (south-eastern United States) using reconstructions of Holocene relative sea level. *J. Quat. Sci.* 29, 749–759.
- Vance, D.J., Culver, S.J., Corbett, D.R., Buzas, M.A., 2006. Foraminifera in the Albemarle estuarine system, North Carolina: distribution and recent environmental change. *J. Foraminifer. Res.* 36, 15–33.
- Watcham, E.P., Shennan, I., Barlow, N.L.M., 2013. Scale considerations in using diatoms as indicators of sea-level change: lessons from Alaska. *J. Quat. Sci.* 28, 165–179.
- Woerner, L., Hackney, C., 1997. Distribution of *Juncus roemerianus* in North Carolina tidal marshes: the importance of physical and biotic variables. *Wetlands* 17, 284.
- Woodworth, P.L., Maqueda, M.Á.M., Roussenov, V.M., Williams, R.G., Hughes, C.W., 2014. Mean sea-level variability along the northeast American Atlantic coast and the roles of the wind and the overturning circulation. *J. Geophys. Res. Oceans* 119, 8916–8935.
- Wright, A.J., Edwards, R.J., van de Plassche, O., 2011. Reassessing transfer-function performance in sea-level reconstruction based on benthic salt-marsh foraminifera from the Atlantic coast of NE North America. *Mar. Micropaleontol.* 81, 43–62.
- Yin, J., Goddard, P.B., 2013. Oceanic control of sea level rise patterns along the East coast of the United States. *Geophys. Res. Lett.* 40, 5514–5520.
- Zaremba, N., Mallinson, D.J., Leorri, E., Culver, S., Riggs, S., Mulligan, R., Horsman, E., Mitra, S., 2016. Controls on the stratigraphic framework and paleoenvironmental change within a Holocene estuarine system: Pamlico Sound, North Carolina, USA. *Mar. Geol.* 379, 109–123.
- Zervas, C., 2009. *Sea Level Variations of the United States 1854–2006*. National Oceanic and Atmospheric Administration, Silver Spring, Maryland, p. 194.
- Zlotnicki, V., 1991. Sea level differences across the Gulf Stream and Kuroshio extension. *J. Phys. Oceanogr.* 21, 599–609.